J. Man, K. Obrtlík and J. Polák: Extrusions and intrusions in fatigued metals. Part 1. State of the art and history

Jiri Man, Karel Obrtlik, Jaroslav Polak

J. Man, K. Obrtlík and J. Polák: Extrusions and intrusions in fatigued metals. Part 1. State of the art and history

Journal:	*Philosophical Magazine & Philosophical Magazine Letters*
Manuscript ID:	TPHM-08-Nov-0447.R1
Journal Selection:	Philosophical Magazine
Date Submitted by the Author:	12-Mar-2009
Complete List of Authors:	Man, Jiri; Institute of Physics of Materials, ASCR Obrtlik, Karel; Institute of Physics of Materials, ASCR Polak, Jaroslav; Institute of Physics of Materials, ASCR
Keywords:	cyclic deformation, defects in solids, dislocation dynamics, experimental, fatigue, polycrystalline metals, slip bands, theoretical
Keywords (user supplied):	persistent slip marking, extrusion, intrusion

REVIEW ARTICLE

Extrusions and intrusions in fatigued metals. Part 1. State of the art and history**

J. Man*, K. Obrtlík and J. Polák

Institute of Physics of Materials, AS CR, Žižkova 22, 616 62 Brno, Czech Republic

(*Received 28 November 2008; final version received xx*)

Current state and historical progress in experimental and theoretical studies of surface relief appertaining to persistent slip bands (PSBs) and leading to fatigue crack initiation in cyclically deformed metals is presented as a thorough critical overview. Comprehensive inventory of microscopic techniques used for this study is tabulated chronologically with accent to their applicability to polycrystals. The most relevant experimental characteristics concerning the surface relief evolution namely the form of extrusions and intrusions in single- and polycrystalline materials are surveyed. Theoretical models and computational simulations of extrusion and intrusion formation and fatigue crack initiation are critically reviewed.

Keywords: persistent slip band; persistent slip marking; extrusion; intrusion; fatigue crack initiation

1. Introduction

The study of the nature and of the physical mechanisms of fatigue damage evolution has been started more than 100 years ago. Ewing and Humfrey [1] in their pioneering work presented optical microscopic observations of the surface of flat specimens of polycrystalline Swedish iron, fatigued in rotating bending. They observed the localized cyclic slip in surface grains and the formation of pronounced surface markings. Their most important finding – the identification of fatigue cracks within the rough surface relief – has activated hitherto persisting interest in this phenomenon. Further important stages in the identification of the mechanisms of the surface relief formation represent the discovery of extrusions [2], intrusions [3–5], persistent slip bands [6], dislocation structure of persistent slip bands [7–9] and its unique relation to sharp surface slip markings [10].

** In 2003 passed 100 years since J. A. Ewing and J. C. W. Humfrey firstly documented the nature of early surface fatigue damage in Swedish iron in their paper "The Fracture of Metals under Repeated Alternations of Stress" published in the journal Philosophical Transactions of the Royal Society of London, Series A [1]. Let this work (Part 1 and 2) commemorates their pioneering effort to understand physical mechanisms of the early fatigue damage.

* Corresponding author. Email: man@ipm.cz

Cyclic plastic strain localization in *persistent slip bands* (PSBs) is now accepted as a general and very important feature of cyclic straining in crystalline materials which can be regarded as the first sign of fatigue damage. The phenomenon of PSBs was discovered by Thompson, Wadsworth and Louat [6] who revealed that locations of the bands remained visible after electro-polishing suggesting that they were structurally different from the surrounding material. Detailed description of their specific dislocation arrangement, identified using transmission electron microscopy [7–10], is beyond the scope of the present review and can be found elsewhere (e.g. [11–17]). At this point, however, it should be noted that the classic well-documented "ladder" structure, schematically indicated in figure 1, is not the only type of dislocation structure that characterizes the PSBs. In some cases, contrary to the clear evidence of cyclic slip localization obtained via surface observations of sharp surface slip markings, there is uncertainty about the internal structure of the respective PSBs so far (compare e.g. [12,13]).

The sharp surface slip markings (formerly named also slip bands, intense slip lines, fatigue deformation markings, fatigue bands, slip striations and/or slip markings) are now called *persistent slip markings* (PSMs). This term emphasizes the well-known fact that surface relief appertaining to PSBs reappear in the same location after the fatigue test had been interrupted, the surface electro-polished, and the test restarted. PSMs are thus manifestation of persistent irreversible slip activity localized within PSBs. PSMs consist of extrusions and intrusions,[1] which develop on the initially flat surface at emerging PSBs (see figure 1), and they are believed to be critical precursors to the nucleation of fatigue cracks (see e.g. [12–17]). Thus the experimental studies on the shape of extrusions and intrusions and the kinetics of their formation can help to find the details of the fatigue crack initiation mechanisms.

[Insert figure 1 about here]

The progress in experimental techniques used for surface relief study, the most relevant qualitative and quantitative experimental data on PSMs, theoretical models and computational simulations of surface relief formation leading to fatigue crack initiation will be reviewed thoroughly in sections 2, 3, 4 and 5, respectively. More emphasis will be put to

[1] The term "intrusion" for a fine crevice-like depression within the PSM has been firstly used by Hull [3]. However, some contemporary authors do not speak about extrusion-intrusion pair and instead they refer to microcrack initiated in the wake of extrusion (see section 4). Although the discussion of fatigue crack initiation is still confronted with a difficulty of the definition of a nucleated crack, some experimental results clearly suggest that there is a difference between intrusion and crack nucleus (see section 6).

polycrystals. The role of surface relief, i.e. the role of PSMs for fatigue crack initiation is discussed in section 6. Importance of experimental data for the understanding of the surface relief formation and its relation to the internal dislocation structure of the PSBs, and for the verification and/or the modification of the existing models of fatigue crack initiation is emphasized in section 7 together with some considerations concerning future development in experimental and theoretical studies in this field.

For the integrity of a discussion, our recent experimental results on simultaneous early growth of extrusions and intrusions obtained by atomic force microscopy (AFM) with respect to the crystallographic orientation of individual grains of 316L steel are also briefly included. They will be however thoroughly presented in part 2 of this paper [20] and compared with theoretical models.

2. Experimental techniques adopted for the study of the early fatigue damage

Microscopic examinations of surface relief evolution and fatigue crack initiation count among experimentally the most demanding studies in fatigue damage of materials. Historically, the advancement of our knowledge concerning the surface relief topography of PSMs and fatigue crack initiation is closely related to the level of experimental techniques. Selected experimental techniques for the study of the surface fatigue damage together with some predictions for future development were summarized by Davidson [21]. Historical evolution of the experimental techniques, manifesting enormous interdisciplinary effort in understanding one of the fundamental phenomena of fatigue during the 100 years period, is chronologically presented in table 1 together with some comments pointing out advantages and/or limitations of each technique. It should be stressed that some specific experimental techniques, based on the optical microscopy (OM) [26] and on the scanning electron microscopy (SEM) [37,40–45], allowing the study of PSM profiles quantitatively, were developed exclusively only for this purpose. For their detailed description the readers are referred to the original papers. Furthermore, it is imperative to note that some of the experimental techniques listed in table 1 are destructive, i.e. they do not permit the sequential observation of one and the same PSM-site during cycling as a function of the increasing number of cycles.

[Insert table 1 about here]

It is evident from table 1 that obtaining detailed information about the surface relief topography and its evolution has been limited for a long time by low resolution of OM. The

only experimental technique enabling to resolve the fine details of the surface relief topography with the help of the OM was taper-sectioning technique [26]. Purely geometrical amplification of the surface profile was achieved by using small taper sectioning angles (less than 10°) after electroplating. In this way the first quantitative information about the growth of extrusions during fatigue was obtained [27]. Later it was demonstrated, however, that the low taper sectioning angle can easily produce artefacts in the observed profiles of extrusions and intrusions [8,28]. Similar profile heights can be obtained nondestructively by using double-beam interferometry. Although this technique is very sensitive to the measurement of height differences (the height of macro-PSMs or slip steps in single crystals) [23,24,71,72], low lateral resolution excludes it practically from the study of individual PSMs in polycrystals.

Considerable progress represented the use of transmission electron microscopy (TEM) in the mid-1950s and even more important step was the introduction of scanning electron microscopy (SEM) in the early 1970s (see Table 1). The study of shadowed two stage plastic-carbon replicas at high resolution in TEM allowed imaging the fine details of surface topography of individual PSMs and revealing of intrusions within PSMs [3]. In spite of the high in-plane resolution (about 5 nm), that can be obtained from plastic-carbon replicas shadowed with a metal for contrast, the out-of-plane measurements (depth of intrusions) lack accuracy and resolution [21]. Nevertheless, the main advantage of this technique, namely the record of surface changes obtained via periodic replication of cycled specimen that allows their storage for subsequent study after crack initiation, is still valid. It is also the reason that the replication technique in conjunction with TEM and/or with OM or SEM at lower resolution or recently with AFM (see below) represents the most enduring technique used for the study of the surface relief evolution and fatigue crack initiation.

The commercialization of the SEM provided a range of magnifications that overlap that of OM and TEM. It is now a standard technique for direct viewing of specimen surface from almost any angle at a wide range of magnifications with no tedious specimen preparation. However, direct examination of the specimen surface in the SEM allows obtaining only a general qualitative picture of PSM topography; the density of PSMs and the density of initiated cracks can be evaluated for different stages of the fatigue life. Fine details of individual PSMs mainly in polycrystals can be imaged by SEM-FEG (high resolution SEM equipped with field emission gun) – see table 1. Due to the specific geometry of PSMs direct examination of the specimen with electron beam perpendicular to the surface can give only partial information [73]. Intrusions or initiated cracks are often hidden below emanating

extrusions (see figure 1) and thus only the tilting of the specimen (electron beam becoming parallel to the active slip plane) can yield more complete information [46,69,70,74]. For obtaining quantitative data on the height of extrusions and/or the depth of intrusions using SEM several special methods were devised (see table 1). Among them two sophisticated techniques provide the most impressive experimental results – section micromilling technique by Hunsche and Neumann [41,42,75] and sharp-corner polishing technique by Basinski and Basinski [43,44,73]. Both methods allow the preparation of cross sections perpendicular to the specimen surface without measurable distortion of the resulting edge and thus provide the sharp true surface profiles of PSMs and initiated fatigue cracks. The Basinskis' technique moreover allows the study of the evolution of PSM profiles and the initiation of fatigue cracks throughout the fatigue life. These techniques are, however, very exacting; they were primarily applied to copper single crystals (only limited data obtained by the section micromilling technique were reported for polycrystalline copper [76,77]) and can hardly be applicable for the systematic study of the evolution of surface profiles in polycrystals. In this context, the very promising method for obtaining similar results also in polycrystals seems to be cross-sectioning technique using FIB (focused ion beam) milling. It was so far adopted for the study of fatigue damage of thin copper films [48] and for the investigation of the small crack behaviour in ferritic-martensitic dual phase steel [49] and the PSMs formation on two mutually perpendicular surfaces in 316L steel [50]. The only technique, that has been used to obtain the quantitative data on the growth of extrusions in polycrystals using the SEM, is the contamination line technique [37,38,78].

In the 1990s, several new microscopic techniques were adopted (see table 1) and among them the atomic force microscopy (AFM) started to be applied most frequently for the quantitative study of surface damage mainly in cyclically strained polycrystals. Its application is still expanding. In spite of some limitations in observation and in quantitative evaluation of PSMs by AFM [67,69,70,74,79] (see table 1), this technique allows obtaining very precise quantitative information on the three-dimensional surface relief. AFM has been employed in the systematic study of the evolution of PSM surface morphology in polycrystals either directly by observing metallic specimen or using plastic replica (for details see [20]). However, in order to obtain true quantitative data on the simultaneous growth of extrusions and intrusions, both observations are necessary [20]. The coupling of AFM with electron backscattering diffraction (EBSD) was shown to represent a very useful combination to reveal crystallographic and topographic aspects concerning the surface relief of PSMs within individual grains of a polycrystal [66,67,79,80].

3. Characteristic features of the surface relief

Surface relief topography has been amply studied in fatigued copper (for review see [12,14, 15,41,73,81]) and in aluminium [58,59] single crystals for which quantitative and qualitative data were collected using various experimental techniques listed in table 1. Similar detailed studies for polycrystalline f.c.c. metals are less numerous [12,41,76,78–80,82]. The most relevant results of experimental investigations concerning the surface relief and its evolution in f.c.c. metals can be briefly summarized as follows:

(i) Morphology of well-developed PSMs differs in single crystals and in polycrystals (see figure 1). Whereas macro-PSMs are typical for single crystals, individual PSMs are present both in single and in polycrystals. Individual PSMs consist of *tongue-like extrusions alternating with intrusions* (mainly at their embryonic stages) or *ribbon-like extrusions* accompanied by intrusions in a characteristic way (cf. figures 2(a) and 2(b)) [8,33,39,47,69, 71,76,78,83–86].[2] Macro-PSMs consist of *protrusions* (by some authors also termed "bulge" or "bulging") with superimposed individual extrusions and intrusions (see figure 2(c)) [39,41, 42,44,58,71–73,81,87–89].

[Insert figure 2 about here]

(ii) Material within one macro-PSB protrudes on two opposite surfaces of a single crystal[3] in the direction of the primary Burgers vector [24,41,71,81,89,90] (see figure 2(c)). TEM observations of subgrain boundary displacement within PSBs on both sides of nickel single crystal by Mecke and Blochwitz [91] demonstrated clearly that PSMs (extrusions) grow in the direction from the interior to the specimen surface.

(iii) Surface relief adjacent to PSBs have a bulk character; i.e. in copper single crystals the height of protrusions is proportional to the width of macro-PSMs [42,87,89] and increases with the depth of the respective macro-PSBs measured in the active slip direction [89,90] and/or with the specimens' thickness [42]. In polycrystalline 316L steel the height of extrusions was found to be proportional to the thickness of the corresponding individual PSB and to the grain size below the surface (i.e. to the depth of PSBs) [80].

[2] In addition to the typical extrusion-intrusion pairs observed most frequently, isolated intrusions were also detected [38,43,73].

[3] Only Ma and Laird [87] reported different type of protrusions in copper single crystals. After quite a large number of cycles they observed that protrusions of heavily deformed macro-PSMs, typically 50 μm in thickness are associated with net inward displacement (i.e. negative protrusions and/or encroachments) on the opposite side of the single crystal. Negative protrusions were also observed on the front-surface in the rectangular aluminium single crystals [58] and in cylindrical copper single crystals at the position where the primary Burgers vector represents a tangent to the specimen surface [89,90].

(iv) Extrusions in polycrystalline 316L steel grow predominantly in the direction of the active Burgers vector; their height is independent of the exact grain orientation relative to the loading axis [80]. In polycrystalline copper the type of activated slip system and its Schmid factor were shown to influence the morphology of extrusions [85].

(v) The initial growth rate of extrusions in polycrystals fatigued at room temperature is high and later drops to a stabilized value [69,78,82,85]. Extrusions can grow continuously during the whole fatigue life in grains in which no cracks develop [82].

(vi) Surface relief of copper single- and polycrystals is formed in a wide interval of temperatures (4.2–533 K). However, the morphology and profiles of PSMs [44,73,83,85,92] and the kinetics of extrusion growth [78,85] are temperature dependent.

(vii) The inert environment (such as vacuum, UHV, nitrogen, argon, helium) has no significant effect on the PSM topography in comparison with the air [33,71,73,75,83,88] but it strongly affects crack nucleation and subsequent crack growth (see for example [73,75]).

This review is limited to the discussion of the surface relief evolution, cyclic slip localization and fatigue crack initiation in f.c.c. metals, however, in spite of some differences in dislocation behaviour in b.c.c. metals broad similarity between b.c.c. alloys and f.c.c. metals has been found. The interested reader is referred to a recent review on this subject [74]. The surface relief and its evolution in fatigued h.c.p. metals has not been studied systematically so far; the only work dealing with this subject in more detail is the paper by Partridge [93].

4. Theoretical models of surface relief formation and fatigue crack initiation

Numerous models involving the formation of extrusions, intrusions and fatigue crack initiation have been proposed. The early models, instigated by the spectacular growth of very thin extrusions in aged Al-Cu alloys [2], were based on the specific irreversible motion of individual dislocations under forward and reversed loading (for thorough reviews see [94–99]). All these models originated before the relevant information on the surface relief and internal dislocation structure in fatigued materials were assessed and they were repeatedly found in conflict with experimental observations.

The latest models of surface relief formation and fatigue crack initiation can be divided according to the underlying mechanisms into three categories (compare [12,14–16,38, 73]). (i) The first group of models considers the details of real dislocation structure of PSBs; fatigue crack initiation in these models is ascribed primarily to the presence of internal stresses within PSBs and their operation at the surface. They are thus called *surface-stress-*

assisted crack nucleation models. (ii) The second group represents *"vacancy" models*. They also consider the dislocation structure of PSBs but are based on irreversibility judged from intra-bulk behaviour of the entire PSB and they emphasize microscopic details of the dislocation processes within the whole PSB. A decisive role in these models is attributed to point defects (vacancies and/or vacancy agglomerates). (iii) The third group of models describing the formation of extrusions and intrusions and fatigue crack initiation represent *micromechanical models*. They neglect the details of dislocation mechanisms within PSBs and are based entirely on the micromechanical considerations under special assumptions or on the energetic arguments. In the following sections 4.1, 4.2 and 4.3 the contemporary existing representatives of all three groups will be presented and critically compared with the actual pertinent experimental data concerning the surface topography of PSMs and its evolution obtained for single- and quite recently also for polycrystals (see section 3).

4.1. *Surface-stress-assisted crack nucleation models*

4.1.1. *Model by Brown and co-workers*

The real dislocation structure of PSBs was taken into consideration for fatigue crack initiation firstly by Antonopoulos, Brown and Winter [19]. The original version of the model by Brown and co-workers [19] has been modified repeatedly (cf. [100–104]). Taking into account the experimental finding [19] that the dipoles in the walls of the PSB and in the matrix are mostly of vacancy type and their density within the PSB becomes much larger than in the matrix, they concluded that the whole PSB layer experiences a macroscopic tensile internal stress[4] in the direction of the primary Burgers vector. To model this internal stresses Brown and co-workers visualized the individual PSB via formation of two extrusions in both ends of the PSB (see figure 3(a)) as a hypothetical vacancy layer in which each wall of vacancy dipoles is replaced by a single immobile fictitious dipole at opposite PSB-matrix interfaces with extra half planes directed into the matrix (see figure 3(b)) [19,100–103]. Thus the PSB is in a state of tension and it provides a driving force for decohesion of the matrix from the PSB. The stress level corresponds to an elastic tensile (so-called fibre) strain of about 2×10^{-4} [19]. No matter how small the tensile strain is, logarithmic infinities in stress are developed at points *A*

[4] It is very little known about the macroscopic stress state within PSB lamellae so far. The only two experimental works on the macroscopical internal stresses within PSBs are in dissent. Ogin and Brown [25] made birefringence observations in optically transparent ionic AgCl single crystals subjected to cyclic loading and their results indicated that PSBs and matrix are in opposite macroscopic stress states which were reversed in signs in each half-cycle. Buque, Tirschler and Holste [105] monitored Barkhausen noise in nickel single crystals cyclically deformed into the saturation stage and they concluded that permanent compressive internal stresses with small cyclic changes exist in PSBs which do not reverse sign during the loading half-cycle.

and B (A' and B') where the interface between the PSB and the matrix meets the external surface of the material [101–103]. The location A is in compression (i.e. crack closing), B in tension (i.e. crack opening) – see figure 3(c). These non-uniform near surface stress fields give rise to the first crack initiation (decohesion) at point B (B') [101–103]. According to Brown [106] there is another driving force, the energy release rate associated with unloading the PSB, and after the crack at B (B') is developed, this can operate to cause decohesion at point A (A'). The initiated cracks are considered to be "dormant" cracks, by Brown [101] also termed Kendall cracks (= the cracks shorter than the Griffith length) which can grow only very slowly by capture of individual dislocations [101–103]. For an individual PSB with the thickness $w < 1\,\mu\text{m}$ (see figure 3(a)) a dormant crack of a length of less than 9.5 μm can be produced [102].

[Insert figure 3 about here]

Taking into account the difficulty of forming an extrusion on the surface according to the scheme shown in figure 3 and the Basinskis' criticisms [73], Brown and Nabarro [104] recently revisited the earlier versions of the model. It is supposed that energy difference between the vacancy and interstitial dipoles of equal height due to nonlinear elasticity is a possible cause of the conversion of interstitial dipoles to vacancy dipoles by slip, with the consequent production of extrusions at the crystal surface. The fibre stress in a PSB is then predicted to be tensile (due to an equilibrium bias in vacancy dipole population) and increases steadily as cyclic straining reduces the average height of the dipoles in the PSB [104].

According to the model by Brown and co-workers [103] the height of the extrusion (see figure 3(a)) is given by the tensile fibre strain ε_f multiplied by the length of the PSB. Thus, for a polycrystal with the grain size D, the height of the static ("athermal") extrusion is expected to be equal to

$$h_e = \varepsilon_f D . \qquad (1)$$

This proportionality is in a qualitative agreement with experimental results [80]. Considering the approximate value of the fibre strain $\varepsilon_f \approx 2\times10^{-4}$ we obtain, however, the heights which are consistent only with the static extrusions formed at the stage of the early rapid growth [69,74,82] but not with the heights observed during continuous steady growth of extrusions within the fatigue life at [69,74,78,82,85,107] and above [78,85] room temperature. The continuous growth of extrusions has not been considered in the model so far but Brown postulates that undoubtedly it will involve some form of vacancy diffusion [106]. For

discussion on the preferential site of the first crack initiation (site *B* or *A*) in an individual PSM according to the model Brown and co-workers see section 6.2.

4.1.2. *Model by Zhai et al.*

Based on the observation of a special configuration of initiated cracks on the side-surface of a rectangular aluminium single crystal containing Burgers vector, Zhai et al. [57,58] suggest that under the combined action of the tensile internal stress and the applied stress (see figure 4(a)), the walls in the PSB may collapse resulting in a large number of vacancies. As a result of aggregation of these vacancies, a microcrack within and perpendicular to the individual PSB and/or alternatively a microvoid may be formed near the surface region (compare figures 4(b) and 4(c)).

[Insert figure 4 about here]

Although the proposed model considers the real dislocation structure of PSB shown in figure 1 it does not respect the state of a dynamic equilibrium between the multiplication and annihilation of both screw and edge dislocations within a PSB (see e.g. [81]) for the considered collapse of the walls near the surface. Furthermore, the model is practically applicable only to the side surface of specially oriented single crystal. The specific configuration of initiated microcracks observed by Zhai et al. on the side surface of fatigued aluminium single crystals after more than 10^6 cycles [58] has not been reported in pure copper single crystals with quite similar geometry so far (see section 3).[5]

4.2. ***Vacancy models***

4.2.1. *EGM-model*

The detailed knowledge of the actual dislocation structure of PSBs together with the consideration of dislocation interactions and vacancy generation gave rise to the well-known EGM-model by Essmann, Gösele and Mughrabi [18] (for further reading see also [38,78,81, 108]). In this model, the surface profile at the emerging PSB is determined by two processes:

[5] It is worthwhile to mention in this context that a similar, unusual configuration of voids and fatigue cracks growing perpendicularly to the PSBs was also observed early by Atkinson (see ref. [103], pp. 194–195) in copper single crystal dispersion-hardened with SiO_2 particles and having the same crystal geometry as shown in figure 4(a). According to Brown [103] these cracks are probably caused by the accumulation of vacancy dipoles at the incoherent interface of the hardening particles (compare also with the model by Hsiung and Stoloff, section 4.2.3).

(1) the rapid formation of a static extrusion [18] and (2) the slow gradual development of surface roughness by random irreversible slip [108].

[Insert figure 5 about here]

EGM-model is based on the analysis of steady-state cyclic deformation in PSBs, involving the dynamic production and annihilation of both dislocations and point defects. The specific sequence of glide and annihilation of edge dislocations within the walls of PSBs proposed leads to a predominance of vacancy-type defects in the PSBs and to the deposition of so-called "interface" edge glide dislocations at opposite PSB-matrix interfaces, as shown schematically in figure 5(a). Extra half-planes of interface dislocations are directed into the PSB and thus the lamella is in a state of compression (contrary to the model by Brown and co-workers – compare figures 5(a) and 3(b)). The number of atoms contained in the extra atomic planes is precisely equivalent to the number of non-equilibrium vacancies in the PSBs in cyclic saturation. Under the action of the applied stress σ, the interface dislocations glide out of the crystal at A and A' during the tensile phases and at B and B' during the compressive phases of cycling, respectively. This process leads to the formation of ribbon-like extrusions emanating out of the PSB (see figure 5(b)) which agrees with experimental findings in single crystals that extrusions grow in the direction from the interior to the specimen surface [91] (see section 3).[6]

Two possibilities for surface relief evolution are considered in EMG model depending on the vacancy mobility:

(i) Static extrusions are expected to develop rather rapidly when the steady-state conditions are reached in the PSB after its formation, i.e. within about 1000 cycles. At low temperature at which vacancies are immobile and cannot migrate from the PSB to the matrix, the growth of extrusions ceases as it was documented for polycrystalline copper [78,85]. Since vacancies are assumed to be formed only in the walls [18,38,78,81] the height of a static extrusion (see figure 5(b)) is expected to be proportional to the relative fraction of the volume of the PSB occupied by the walls f_{w}, to the saturated vacancy concentration in the walls $C_{\mathrm{v}}^{\mathrm{sat}}$ and in case of a single crystal to the specimen diameter D (see figure 5(b))

$$h_{\mathrm{e}} = \frac{f_{\mathrm{w}} C_{\mathrm{v}}^{\mathrm{sat}} D}{2}. \qquad (2)$$

An upper limit for the initial (static) extrusion growth rate can be given as [78,81]

[6] At this point it should be pointed out that the formation of intrusions by analogous mechanism sketched in figure 5 is excluded in EGM model [17,18].

$$\frac{\mathrm{d}h_\mathrm{e}}{\mathrm{d}(\Delta N)} \le f_\mathrm{w}\rho_\mathrm{e}^\mathrm{sat} y_\mathrm{e}^2 c_\mathrm{e}\gamma_\mathrm{pl,PSB} D \qquad (3)$$

where $\rho_\mathrm{e}^\mathrm{sat}$ is the local density of edge dislocations in the dipolar walls of the PSB, y_e is the annihilation distance for two unlike edge dislocations, c_e is the fraction of plastic strain carried by edge dislocations in the PSB, $\gamma_\mathrm{pl,PSB}$ is the local plastic shear strain amplitude in the PSB and ΔN is the age of the PSB (number of cycles after its formation). Using typical values for the parameters in equation (3) for copper, an upper limit of the rate of static extrusion growth is estimated as ca. $4.75\times10^{-6} D$ nm cycle^{-1} [78].

In case of a polycrystal the EGM concept is quite similar, except that D in equation (2) denotes the grain size and the whole extrusion (with twofold height) emerges at the free surface on one side of the PSB since the other side is blocked by the grain boundary.

The proposed proportionality with D agrees with experimental results obtained not only for single crystals (see section 3) but also recently for polycrystalline 316L [80]. The emergence of a static extrusion can be also clearly recognized in a short period of initial rapid growth of extrusions during about 500–900 cycles. It was experimentally detected in two polycrystalline steels fatigued at room temperature [69,74,82]. Quantitative data concerning the initial growth of static extrusions both for copper [78] and for steels [74,82] are consistent with the limitation set by EGM-model (equation 3).

(ii) At higher temperatures at which vacancies are mobile, EGM model also considers the possibility vacancy migration from the PSB into the matrix. However, according to them and contrary to Polák's model (see section 4.2.2) vacancies can flow effectively to the matrix only from a very thin layer (~ 5–10 nm) of the walls [18,38]. This mechanism can give rise to two thin (<0.1 μm) continuously growing extrusions at both PSB-matrix interfaces. Such thin extrusions are typical for age-hardened alloys but not for pure f.c.c. metals (see figure 2(a)).

In addition to the rather rapid formation of static extrusions the slow roughening of static extrusions by random glide processes later in the fatigue life results in the final profile of extrusions – see figure 5(c). For the case of an individual PSB it will be discussed below in model proposed by Differt et al. [108] (see section 5.1).

The initiation of stage-I shear cracks is proposed by decohesion that is triggered in the notches (i.e. stress raisers) of the rough surface topography. Two distinct types of stress raisers considered by EGM are indicated in figure 5(c) [18,38,82]. The slip offsets at the PSB-matrix interface (Type I stress raisers) form early (see figure 5(b)), whereas the notch-like valleys in the roughness profile of the PSM (Type II stress raisers) develop gradually, much

later in fatigue life (see figure 5(c)). The proposed scheme can be reconciled with experimental results obtained for individual PSBs in single crystals and partially in polycrystals [38]. However, it can hardly explain the early appearance and growth of parallel intrusions at both PSB-matrix interfaces in fatigued polycrystalline 316L steel [20].

4.2.2. *Polák's model*

An important extension of EMG model stimulated by the observations of the detailed form of extrusions and intrusions in copper single crystal [39] represents the model proposed by Polák [109] (for further reading see also [12,69,110,111]). The model is based on the same dislocation arrangement and dislocation motion but point defects are supposed to be generated in the whole volume of a PSB, i.e. both in dislocation-rich walls and in dislocation-poor channels (see figure 1). Two basic mechanisms of point defect formation were considered by Polák [112]: mutual annihilation of two opposite edge dislocations moving on neighbour planes and non-conservative motion of a jog on a screw dislocation. Using energy arguments, in accordance with the EGM-model, vacancy production is preferred. The rows of vacancies can be disintegrated by thermal activation or by intersection with moving dislocations and mobile vacancies or di-vacancies in non-equilibrium concentrations are produced. The rate of vacancy production in the whole volume of PSB at room temperature was evaluated from resistivity measurements in copper single crystal fatigued at liquid helium temperature approximately to 2.5×10^{-6} cycle^{-1} [113].

[Insert figure 6 about here]

Since vacancies or di-vacancies are mobile at room temperature, they will migrate and annihilate when approached to sinks. The vacancy production rate is approximately homogeneous within the PSB, however, the annihilation rate is a function of sink density. Since edge dislocations and edge dipoles are perfect sinks for vacancies and their density is much higher in the walls than in the channels, the specific inhomogeneous quasi-equilibrium vacancy concentrations arise as a consequence of the dynamic equilibrium between the production and the annihilation of vacancies during constant frequency cycling (see figure 6(a)). The vacancy concentration reaches maximum in the middle of the channels (compare sections $A-A'$ and $B-B'$) and decreases towards the walls (see section $A-A'$) and the matrix (see section $B-B'$). The arising concentration gradients result in a systematic flux of vacancies from the channels to the walls and/or to the surrounding matrix as depicted in figure 6(a). This results in a net flow of atoms in the opposite direction, i.e. mass

redistribution. In dependence on the prevalent fraction of mass redistribution – within PSB and/or across PSB-matrix interface – two basic different morphologies of individual PSMs are predicted by Polák [12,109].

The flux of vacancies from the channels to the walls within the PSB results in the accumulation of the mass in the channels and its diminution in the walls. Compressive and tensile stresses, respectively, built up due to this mass redistribution, can be continuously relaxed only in the x-direction (see figure 6(a)) [12,109]. This leads to the gradual production of extrusions at the sites where channels intersect the surface and intrusions where walls intersect the surface, i.e. tongue-like extrusions alternate quasi-periodically with intrusions along a PSM (compare figures 6(b) and 2(a)). The average spacing s between the tongue-like extrusions (or intrusions) at the early stage of PSM development is given by [39]

$$s = \frac{d}{\cos\alpha} \tag{4}$$

where d is the mean spacing between the walls in the PSB and α is the angle between the primary Burgers vector and the intersection of the primary slip plane with the surface (see figure 6(b)). The experimental observations on copper single crystal are in agreement with the proposed prediction [39]. Only partial validity of equation (4) was found for individual grains of polycrystalline copper fatigued at 107 K [85].

More important for crack initiation is the mass redistribution between the PSB and the matrix. Due to this redistribution, the mass accumulates in the whole PSB and diminishes within a thin layer of the matrix close to the PSB-matrix interface where the vacancies are absorbed by edge dislocations. The mass redistribution results in the build up of compressive stress in the PSB lamella. This compressive stress is continuously relaxed by gliding dislocations, however only in the direction of the active Burgers vector. This leads to the steady growth of a ribbon-like extrusion the width of which corresponds to the width of the respective PSB (see figure 6(c)). Due to mass reduction close to the PSB-matrix interfaces the tensile macroscopic stresses arise and are relaxed by moving dislocations. As a result narrow intrusions originate and their depth increases progressively.

The process of formation central ribbon-like extrusion accompanied by two parallel intrusions has been formulated by Polák recently [110] in terms of the vacancy production rate $p(\varepsilon_{ap})$, which depends on the local plastic strain amplitude and vacancy annihilation rate A due to the sweeping of vacancies by moving dislocation loops. The vacancies disappear from the PSB also by migration to the matrix. The net change of vacancy concentration in a cycle is

$$\frac{\mathrm{d}c}{\mathrm{d}N} = p(\varepsilon_{\mathrm{ap}}) - (A + M(T))c \tag{5}$$

where $M(T)$ is the vacancy migration rate characterizing the flow of vacancies out of the PSB to the matrix (fraction of vacancy concentration leaving the PSB-matrix boundary). The relative annihilation rate is independent of temperature but the vacancy migration rate is strongly temperature dependent and is determined by the vacancy diffusion coefficient and geometrical parameters.

General equation (5) was recently solved by Polák and Sauzay [111] for the simplified case of isolated PSB having the width w whose interface with the matrix represents perfect sink for vacancies. The profile of vacancy concentration in x direction across the band was

$$c_{\mathrm{v}} = \frac{p}{A}\left[1 - \frac{\cosh(ax)}{\cosh(aw/2)}\right] \tag{6}$$

where $a = \sqrt{A/D_{\mathrm{v}}\tau}$, D_{v} is the vacancy diffusivity, and τ the period of the cycle.

Considering the flow of atoms from the matrix to the PSB is equal to the net flow of vacancies from the PSB to the matrix the steady growth rate of the extrusion height was derived

$$\frac{\mathrm{d}h_{\mathrm{e}}}{\mathrm{d}N} = \frac{2pL}{w}\sqrt{\frac{D_{\mathrm{v}}\tau}{A}}\,\mathrm{tgh}\left(\frac{w}{2}\sqrt{\frac{A}{D_{\mathrm{v}}\tau}}\right) \tag{7}$$

where L is the depth of the PSB below the surface. The growth rate of the extrusion is proportional to the vacancy production rate and depends on the vacancy diffusivity.

The simplified model cannot yield the growth kinetics of intrusions, however, intrusions arise at the PSB matrix interface, considered in the solution of Polák and Sauzay as a perfect sink. It is proposed that only vacancies from the channels of the PSB can reach the matrix and contribute to the growth of extrusion and deepening of intrusions. In constant plastic strain amplitude loading at temperature at which vacancies can migrate, after the initial delay, a linear growth of an extrusion and two parallel intrusions is thus expected. This is in good qualitative agreement with the kinetics and the details of surface geometry of PSMs presented in the part 2 of this paper [20]. Intrusions are supposed to play a decisive role in fatigue crack initiation as discussed in section 6.2.

4.2.3. *Model by Hsiung and Stoloff*

An important role of the vacancy migration is attributed in the specific model by Hsiung and Stoloff [114]. Based on the observations of vacancy clusters by TEM and SEM at and beneath

the surface of Ni_3Al+B single crystals fatigued at room temperature they suggested that lattice misfit develops between the PSB and the matrix. The misfit strain at the PSB-matrix interfaces is considered to increase with increasing cumulative plastic strain. The condensation of vacancies at interfaces leads to the formation of microvoids (microcracks) at PSB-matrix interfaces. The microvoids break down the coherency between the PSB and the matrix and thereby relieve the accumulated coherent misfit strain at the interfaces. Based upon a surface energy criterion and considering the misfit strain and the critical size of vacancy clusters (i.e. intrusions at the surface) for nucleation of a stable crack they derived the equation for the number of cycles to crack initiation in air and in vacuum. In both cases the number of cycles for crack initiation is inversely proportional to the excess-vacancy generation rate in PSBs [114]. The model does not require prior surface roughening (i.e. formation of extrusions and intrusions) although it implies that extrusion-intrusion pairs may be a product of short range vacancy migration and mass transfer. Furthermore the model was suggested specifically for Ni_3Al single crystals in which no PSBs with typical ladder structure (see figure 1) were observed. The fact that no clear voids due to the condensation of vacancies have been convincingly detected beneath the surface of pure copper single crystals at least at room temperature (compare for example [44,75,87]) throws some doubts on the general applicability of the above model.

4.3. *Micromechanical models*

4.3.1. *Model by Lin and associates*

The basic idea of this micromechanical model is that the extrusions and/or intrusions are driven by alternate specific micro-stress fields in the PSBs. Lin et al. [99,115–117] elaborated these micro-stress fields analytically and computed the relevant plastic shear strains in PSBs accumulated during cycling. The amount of cumulative "creep" plastic shear strain at the surface is taken as a measure of the extent of extrusion and/or intrusion. The model was initially considered only for a polycrystal [99,115–117] and recently was also applied to single crystal [117,118].

[Insert figure 7 about here]

To illustrate the ratchet mechanism, a PSB is modelled as a thin slice R sandwiched by two thinner intensively deformed PSB-matrix interface slices P and Q, as shown in figure 7(a) [115–117]. The slices lie parallel to the slip direction in most favourably oriented grain of a

polycrystal. Further assumption is that a specific initial stress field τ^{i} near the free surface exists in slices P and Q due to lattice imperfections. For the pushing of material in slice R out of the free surface, i.e. for the formation of an extrusion, a favourable distribution of initial shear stresses is required to be positive in P and negative in Q (see figure 7(b)).[7] An intrusion is produced when the signs in P and Q are reversed (see figure 7(c)).

During loading, when the shear stress reaches the critical shear stress τ^{c}, slip occurs to give plastic shear strain $e''_{\alpha\beta}$. After unloading, this slip remains and causes a residual shear stress τ^{r}. Under a given loading the total resolved shear stress τ consists of three components as follows:

$$\tau = \tau^{i} + \tau^{a} + \tau^{r} \tag{8}$$

where τ^{a} is the resolved shear stress in the primary slip system due to the applied load σ_{22}. The governing condition to initiate or to continue sliding is

$$\tau = \tau^{c} \text{ slip occurs} \qquad \tau < \tau^{c} \text{ no slip}. \tag{9}$$

Following the equations (8) and (9), the sequence of alternate micro-stress fields in P (τ_{P}) and Q (τ_{Q}), which promotes the formation of extrusion in R, is further explained by Lin et al. as follows [118]:

(i) During the first forward loading ($\tau^{a} > 0$) P slides, the residual shear stress in P $\tau^{r}_{1fP} < 0$. We have

$$\begin{aligned} \tau_{P} &= \tau^{i}_{P} + \tau^{a} + \tau^{r}_{1fP} = \tau^{c} \\ \tau_{Q} &= \tau^{i}_{Q} + \tau^{a} + \tau^{r}_{1fQ} > -\tau^{c} \end{aligned} \tag{10}$$

where the subscript "1" denotes the loading cycle and f the forward loading.

(ii) During the first reverse loading ($\tau^{a} < 0$) Q slides, the residual shear stress in Q $\tau^{r}_{1rQ} > 0$. We have

$$\begin{aligned} \tau_{P} &= \tau^{i}_{P} + \tau^{a} + \tau^{r}_{1fP} + \tau^{r}_{1rP} < \tau^{c} \\ \tau_{Q} &= \tau^{i}_{Q} + \tau^{a} + \tau^{r}_{1fQ} + \tau^{r}_{1rQ} = -\tau^{c} \end{aligned} \tag{11}$$

where the subscript r denotes the reverse loading. The critical shear stress τ^{c} is assumed to be constant, i.e. no strain hardening or softening is involved. This process is repeated for each loading cycle and gives the natural gating mechanism to cause alternate sliding in P and Q. As

[7] Lin and Ito [115] intuitively suggested that the initial stresses in P and Q may be provided by a row of interstitial dipoles along slice R in the same visual fashion as considered later by EGM (see figure 5(a)), i.e. slice R is in the state of compression. The only experimental evidence documenting indirectly the particular distribution of initial shear stresses in P, Q and R is that by Wood and Bender [119] who studied slip band displacement across artificial scratches in copper subjected to alternate torsion (see also [99,117]).

a result, positive slip in P and negative slip in Q increase monotonically with loading cycles, and produce quickly a static extrusion during the first few hundred loading cycles [115–117]. Then, the static extrusion can continue to grow considerably, however, only if the activation of secondary slip system is considered [116,117].

The kinetics of extrusion growth predicted by this model is in a reasonable agreement with experimental results on f.c.c. polycrystals [69,78,82]. The thickness of PSBs considered in this model (0.1 μm) is typical for age-hardened alloys and is much smaller in comparison with the typical value observed in f.c.c. metals (compare figures 2 and 7). Numerical calculations of a static extrusion in aluminium polycrystal for dimensions of the slices P, R and Q and the linear dimension (grain size) $d = 50\,\mu\text{m}$ shown in figure 7(a) yield the height only of 1.28 nm [116,117]. This value seems to be considerably underestimated in comparison with experimental results on f.c.c. polycrystals [69,78,82]. The occurrence of the secondary slip was evidenced by the study of dislocation structures [120–123] and by surface observations [58,124]. However, it is difficult to expect that the activation of secondary slip system, necessary for continuous growth of extrusion beyond the static extrusion, will occur after 500 cycles as considered in the model by Lin and associates [116,117]. The main handicap of this model is that it considers the formation of either extrusion or intrusion depending on the sign of the initial stress field (see figure 7) and thus it is not able to explain simultaneous growth of extrusions and intrusions in an individual PSM as observed recently [20].

4.3.2. *Model by Mura and co-workers*

The basic idea of this model is dislocation accumulation alternating between two parallel very closely located layers during loading stress cycle. The monotonic build-up of dislocation dipoles piled up against an immobile obstacle (i.e. grain boundary) is associated with the progress of extrusion or intrusion. The number of cycles to fatigue crack initiation in the form of Coffin-Manson law is derived using energy consideration [125–128].

[Insert figure 8 about here]

Tanaka and Mura [125] consider the most favourably oriented grains located at the surface (the slip plane normal and the slip direction are inclined at 45° to the stress axis). Figure 8(a) shows the grain with three isolated individual PSBs (visualized by very thin plate-

like layers) in the section perpendicular to the specimen surface.[8] Dislocations are generated at the specimen surface and move to the interior of a grain. Forward loading causes a pile-up of dislocation with a positive sign on layers I; the reverse flow is taken up by the dislocation with a negative sign moving on neighbour layers II which are located very close to the layers I. The ratchet deformation is enhanced by the help of back stress due to dislocations from the previous segment of loading cycle. In this way, the accumulation of dislocation dipoles is amplified with the number of cycles. Due to accumulation of vacancy or interstitial dipoles (see figure 8(a)) an extrusion or an intrusion is monotonically built up. An extrusion-intrusion pair can be formed when the negative dislocation motion takes place on two layers adjacent to layer I as shown in figure 8(a) [125]. According to Tanaka and Mura [125] there are two ways for the formation of an embryo of fatigue crack for configuration shown in figure 8(a). Growing tensile stress built up with the number of cycles between two layers at the top of pile-up of vacancy dipoles becomes large enough to create the nucleus of a crack suddenly when the fracture criterion is satisfied. In case of extrusions, embryonic cracks are thus formed inside the material at the grain boundary of a surface grain where the vacancy dipoles are piled-up (compare figures 8(a) and 8(b)). The formation of an intrusion causes the stress concentration under the applied stress and it can be also regarded as the crack embryo (compare figures 8(a) and 8(c)). The following growth of a crack embryo is expected to take place along the slip bands – see figures 8(b) and 8(c).

The crack of the grain size arises at the number of cycles N_n (crack nucleation life) when the stored elastic strain energy of accumulated dislocations reaches a critical value. Using the theory of continuously distributed dislocations Tanaka and Mura derived the following relation [125]:

$$N_n = \frac{4Gw_s}{(\Delta\tau - 2k)^2 \pi(1-\nu)d} \tag{12}$$

where G is the bulk shear modulus, w_s the specific fracture energy, $\Delta\tau$ the resolved shear stress range, k the frictional shear stress, ν the Poisson's ratio, and d the grain size. The model thus predicts that the nucleation life is inversely proportional to the grain size.

Original version of the model was repeatedly modified later (compare [125–128]). Venkataraman et al. [126] considered the inclination of an isolated PSB (visualized by vacancy dipoles) to the specimen surface and included the effect of temperature and environment. They used a free-energy criterion to predict crack nucleation along PSBs. This

[8] The second extreme case of the most favourably oriented grain considered by Tanaka and Mura [125] and later by Chan [128] is that with the slip direction parallel to the specimen surface. In this case however no extrusions or intrusions are formed by dislocation accumulation during cycling and thus it is not presented here.

model was later extended by Venkataraman, Chung and Mura [127] to include multiple mutually interacting slip bands visualized by vacancy dipoles and the effect of random slip. Coffin-Manson type law for crack nucleation has been derived [129]. Chan [128] modified the model to include the influence of microstructure.

Although the formation of extrusions or intrusions is included into the model by Mura et al. the main attractiveness of the model lies in the possibility of quantitative evaluation of the crack nucleation life in relation to some primitive microstructural parameters. The mechanism of crack nucleation shown in figure 8(b), primarily considered in the model, can be however hardly reconciled with the available experimental data. It is generally accepted that fatigue cracks start at the surface in the vicinity of extrusions (see figure 2) and not beneath the specimen surface at the grain boundary. Furthermore, the equation (12) could be derived only when the layers I and II are located very close to each other [125], i.e. for very thin PSBs (2 nm [126]). This value is not compatible with the typical value observed in f.c.c. metals (see figure 2). The main criticism is, however, that the model is applicable only to polycrystals where the immobile obstacles, i.e. grain boundaries are present. The model is not thus capable to explain the surface relief formation and fatigue crack nucleation in pure, notch free single crystals.

4.3.3. *Other (micromechanical) models*

Basinski and Basinski [44] performed extensive study of profiles of macro-PSMs (protrusions) in copper single crystals fatigued at temperatures in the interval 4.2 to 350 K using sharp corner technique.[9] They concluded that there is no correlation between macro-PSM morphology and point defect mobility. It has cast some doubt on vacancy models (see section 4.2) and thus Basinski and Basinski, inspired by observations of shape changes during tension and/or compression, suggested that slip on secondary slip systems with Burgers vectors lying in the cross-glide plane may be responsible for observed macro-PSMs profiles [73,130]. A simple calculation indicates that a minute fraction of the cumulative strain occurring on secondary slip system could account for the largest observed protrusions [73]. The authors, however, concluded that although secondary slip can occur through the temperature interval 4.2–350 K it is not clear how it could account for the temperature changes of macro-PSM profiles, observed also at 15 K [73].

[9] It should be noted that copper single crystals used for the study in the mentioned temperature interval were pre-fatigued with plastic strain amplitude of $\pm 2\times10^{-3}$ or $\pm 1\times10^{-3}$ at room temperature to about half the saturation stress [44].

[Insert figure 9 about here]

The original so-called crack closure-fracture surface rubbing (CCFSR) mechanism of formation of extrusion was offered by Dickson et al. [131] (for detail description of the model see also [14]).[10] They postulate that the intrusions and later microcracks are formed first within the channels of a PSB (probably by sweeping of edge dislocation vacancy dipole loops to the free surface). As soon as the microcracks are present in a material, thin (~0.1 μm) tongue-like extrusions start to form by the CCFSR mechanism schematically shown for a single crystal in figure 9. Then they can grow into relatively long ribbons [131]. The simple scenario proposed by Dickson et al., i.e. extrusions come after the crack initiation, however, is in contrast with the experimental results obtained recently in polycrystalline 316L steel [20]. Furthermore, the CCFSR mechanism proposed on the basis of observations of surface and partly-opened cracks in Cu and 70Cu-30Zn polycrystals is not able to explain the temperature dependence of the kinetics of extrusion growth experimentally found for copper [78,85]. Admitting some possibility of extrusion formation by CCFSR mechanism in case of a stage I fatigue crack, there is no explanation of experimentally observed growth of much wider extrusions since the onset of cycling [74,82] when neither intrusions nor initiated cracks are present in individual PSMs [20].

5. Computational modelling of surface relief formation and fatigue crack initiation

Similarly to the theoretical models, computational simulations of surface roughness evolution and fatigue crack nucleation are also based on various physical principles including slip irreversibility. Most of them reflect the details of dislocation mechanisms within PSBs and use the actual structural and material parameters for the two-dimensional and quite recently three-dimensional modelling of surface relief evolution by various computational methods.

5.1. *DEM-model*

In addition to the evolution of static extrusion (see section 4.2.1) slow surface roughening produces the final profile of PSMs in EGM model (see figure 5(c)). Random irreversible glide processes leading to the surface roughening were considered in quantitative form by Differt, Essmann and Mughrabi (DEM) [108]. Their model is based on the knowledge of overall slip irreversibility p_{PSB} inferred from a statistical treatment of screw dislocation behaviour within

[10] Similar 'ratcheting' mechanism whereby extrusion-intrusion pairs are formed at pre-existing stage I cracks has been already considered in a more general form by Neumann, Fuhlrott and Vehoff [132].

PSBs performed by Essmann [133]. Considering the existence of a dynamic equilibrium between dislocation multiplication and annihilation in PSBs Differt et al. studied the evolution of the average surface roughness due to accumulation of irreversible microscopic positive and negative slip steps at the surface using computer simulation of surface profiles of an individual PSB. The kinetics of the development of the mean depth $\overline{w}$ (peak-to-valley) of the roughness profile in the direction of the primary Burgers vector can be approximated by [108]

$$\overline{w}/b = f(4Np_{\mathrm{PSB}}\gamma_{\mathrm{pl,PSB}}h/b)^{1/2} \tag{13}$$

where b is the magnitude of the Burgers vector, f is a non-dimensional factor, N is the number of cycles, p_{PSB} is the ratio of the irreversible strain to the total strain within the PSB, $\gamma_{\mathrm{pl,PSB}}$ is the local plastic shear strain amplitude in the PSB, and h is the thickness of the PSB. Considering the typical values in copper, equation (13) can be rewritten in simple form [38]:

$$\overline{w} \approx 1.5\times10^{-3}(\Delta N)^{1/2}\ [\mu\mathrm{m}] \tag{14}$$

where ΔN refers to the number of cycles after the PSB has been formed. It should be stressed that equations (13) and (14) are valid only as long as individual PSBs with a typical thickness of 1 μm are considered. As follows from equations (13) and (14) the roughness increases as the square root of the cycle number, i.e. the roughness effect will be detectable after sufficiently extended cyclic deformation (more than 10^5 cycles are required in order to generate surface roughness within an individual PSM with a mean profile depth $\overline{w} \approx 0.5\,\mu$m [38]).

Very good agreement between roughness profile observed experimentally and generated by DEM-model was found for fatigued planar-slip Cu-30at.%Zn single crystals [38]. In the case of copper single crystals the prediction of the DEM model can be reconciled with the experimental observation of the surface profile of "old" extrusions at 77 K [78,108]; at higher temperatures the surface profiles of extrusions become complex and the assumption of random slip leading to surface roughness is unrealistic [78]. In the case of polycrystals, agreement with the DEM model was found for individual PSMs with a rather rugged hill-and-valley surface topography observed by Mughrabi and his co-workers in copper with average grain size of 25 μm [37,38]. Very fine surface structure of extrusions observed by SEM-FEG in austenitic [46,70,82] and ferritic [74] stainless steel correspond to the random fine slip and can be also reconciled with DEM model. Generally, in spite of the variability in morphology of PSMs observed in polycrystalline copper, DEM model cannot explain the typical shape of

extrusions shown schematically in figure 2 and in particular their continuous growth reported not only in polycrystalline material (see section 3).

5.2. *Model by Rosenbloom and Laird*

Computer model of macro-PSM notch-peak topography evolution by Rosenbloom and Laird [134] represents the concept of random relative motion of parallel cards considered much earlier by Wood [26] and later in quantitative form using statistical considerations by May [135,136]. The model is based on the detailed interferometric surface cycle-by-cycle study of macro-PSM behaviour in copper single crystals which showed that not all slip planes active over the course of the fatigue cycling are active during each half-cycle [134]. Then the evolution of surface roughening of a macro-PSB (and not of an individual PSB) is simulated as a superposition of elementary positive and negative slip steps (increments) created during tension and compression half cycles.

Rosenbloom and Laird in their model consider a macro-PSB 60 μm in thickness (see figure 2) consisting of 60 cards which represent 1 μm thick individual PSBs. The fraction of active slip cards during each half cycle was 0.85; the choice of the active slip card is random after assuring that each chosen slip card has received at least one increment of slip step with a height of 0.005 μm and the total displacement was consistent with the applied strain. In simulated profiles of a macro-PSM the presence of a 4 μm peak or 4 μm valley is then used as a crack initiation criterion because according to Rosenbloom and Laird, ideally, a 4 μm peak on one side of the crystal would be equivalent to a 4 μm valley on the opposite side.

The number of cycles required to reach a 4 μm peak or valley was computed in the interval of about 455–3459 cycles. By adding 2000 to 5000 cycles necessary for achievement of the saturation they thus obtained the interval of 2455–8459 cycles required for crack initiation in copper single crystal for the amplitudes in the mid-region of the plateau of the cyclic stress-strain curve [134]. Although this interval of cycles is in good agreement with experimental findings obtained by Ma and Laird [137] the profiles of macro-PSMs generated by the random slip model can be hardly reconciled with the systematically observed shape of macro-PSMs consisting typically of a protrusion with superimposed individual extrusions and intrusions (see figure 2(c)). Accordingly, Rosenbloom and Laird [134] admit the possibility of vacancy-produced protrusion on which the generated roughness is superimposed. The main handicap of the model is, however, that it cannot explain the experimental fact that PSMs grow in the direction from the interior to the surface of a single crystal [91] resulting in the geometry of macro-PSM shown in figure 2(c). Negative protrusions (valleys in the model)

considered as a crack initiation criterion are not a general surface feature of macro-PSMs and they were observed on the opposite side of a macro-PSB after quite large number of cycles (see section 3).

5.3. *Model by Repetto and Ortiz*

Repetto and Ortiz [138] adopted the mechanisms of dislocation interactions, point defect production and their migration towards to the free surface and performed two-dimensional finite element modelling (FEM) of formation and growth of extrusion and intrusion in nominally defect-free pure f.c.c. metals. They consider a fully formed individual PSB imbedded in the matrix in a copper crystal oriented for single slip with dislocation structure shown schematically in figure 1. Annihilation of two opposite edge dislocation segments in the walls of PSBs, when the separation of two segments is smaller than 1.6 nm results in vacancy generation. According to the authors another effect of dislocation annihilation is a steady elongation of the PSB along the nominal slip plane via dislocation climb. Furthermore, Repetto and Ortiz consider the vacancy migration, facilitated by the pipe diffusion along screw dislocations, to the surface. The shape of surface profile of a PSM is determined by the competition between these two mechanisms: the lengthening of the PSB which pushes material out of the matrix, and the vacancy flux through the surface, which causes the surface to recede. The former process dominates in the centre of the PSB which facilitates the formation of a hilly extrusion. The inward motion of the surface is expected to be most pronounced at the PSB-matrix interfaces, and thus results in groove formation at sites where an extrusion emerges on the surface. These grooves (especially the groove at the side *B* of an extrusion – see figure 2) sharpen steadily to form a mathematically sharp crack (the angle at the apex is close to zero).

Very good agreement can be found between the extrusion profile for copper single crystal computed by Repetto and Ortiz [138] and that observed at 77 K by Differt et al. [108]. The kinetics of the typical extrusion growth predicted by this model is however different from experimental results obtained for copper single crystal [78] and for f.c.c. polycrystals [69,78,82] with much smaller grain size than the PSB length considered by Repetto and Ortiz. The kinetics of the groove depth growth seems to be unrealistic in the light of the experimental results (see e.g. [20,43,83,92]). After 65 000 cycles Repetto and Ortiz obtained for a copper single crystal fatigued with plastic strain amplitude of 6×10^{-3} a groove with the depth of 14 nm [138]. Moreover, the basic considerations on which the model is based do not correspond to the knowledge of the annealing kinetics of point defects (see e.g. [139]). Point

defects anneal not only to the outer surface of the crystal but every edge dislocation and/or edge dipole serves as a perfect sink for mobile vacancies. The high vacancy type dipoles cannot be considered as mobile vacancy defects. The maximum height of dipole that can be dispersed into mobile single and di-vacancies is one atomic distance; i.e. it represents a row of vacancies. Thus the dipoles with the height higher than one atomic distance, up to 1.6 nm, considered by Repetto and Ortiz [138] as point defects, are very difficult to disintegrate into mobile defects and should be considered as a part of dislocation substructure.

5.4. *Discrete dislocation dynamics (DDD) modelling*

The novelty in computational modelling of fatigue crack initiation is the use of two- (2D) [140,141] and/or three-dimensional (3D) [142–144] discrete dislocation dynamics (DDD) method. In DDD method, dislocations are generally modelled as line singularities in an elastic solid where they are generated from pre-existing dislocation sources and can glide or annihilate. The description of the plastic deformation directly emerges from the collective effect of a large number of discrete dislocations. Constitutive rules for characterization of their behaviour are implemented explicitly. In the following only the basic assumptions will be given; for detail description of DDD formalisms the reader is referred to the original papers.

Brinckmann and Van der Giessen [140,141] considered 2×2 μm surface grain with three slip systems (60° from each other); the primary slip system was oriented at 45° to the applied cyclic load. All dislocations considered for plastic flaw inside the grain were of edge character with the Burgers vector in the plane of the model. In addition to mutual annihilation dislocations can escape from the grain at the free surface. Brinckmann and Van der Giessen using 2D DDD simulations calculated the stress profiles near the surface to check the presence of logarithmic stress singularities considered for fatigue crack initiation in the model by Brown and co-workers (see figure 3(c)). Their simulations revealed mostly tensile stress along the surface as well as the change of the stress with continuing cycling, but no sign of a logarithmic singularity even after 2000 cycles [140,141]. At this number of cycles, however, no evidence of clear well-defined dislocation structure could be found [140].[11]

Déprés, Robertson and Fivel [142–144] recently performed 3D DDD modelling of early fatigue damage in surface grains of 316L steel at 300 K. Their model is based on an edge-screw fragmentation of the dislocation segments with possibility of cross-slip of screw

[11] The grain size considered in the computer simulations by Brinckmann and Van der Giessen is very close to the minimum grain size of about 1 μm and less which was found to be a limit for formation of PSBs with ladder structure [145] and/or any dislocation patterning [146].

segments. Surface grains in the shape of a cylinder or a half-dodecahedron with diameters within the range 10–22 μm were considered. Dislocations generated from individual Frank-Read sources are free to escape on one top surface whereas all others surfaces act as strong obstacles. Point defects, dislocation climb and environmental effects were not taken into account. Cyclic loading conditions were imposed in terms of constant plastic strain amplitude.

Déprés et al. simulated the formation of dislocation structures [142] and surface relief of PSMs [144] and they also formulated micro-crack initiation model. They obtained PSBs of 200–500 nm in the thickness with an original morphology involving immobile inter-channel tangles, highly mobile pile-ups at the PSB-matrix interfaces and potentially mobile multi-polar walls inside the channels (i.e. chimney-like arrangements of regularly spaced multi-poles made of prismatic loops with the same area as the channel cross-section) [142]. The interaction between the activated primary slip system and the associated cross-slip system was found to be crucial in the formation of these PSBs. In addition to the reversible unidirectional slip steps associated with the early formed pile-ups, true PSMs appear and grow in areas where PSBs with original structure intersect free surface. According to Déprés et al. [144] their growth is associated with the emergence of the potentially mobile multi-polar dislocations located within the channels. PSMs consist of mostly tongue-like extrusions and less numerous intrusions. In agreement with experimental results [80] the height of extrusions was found to be a linear function of the grain size [144]. Based on the analysis of dislocation distortion energies Déprés et al. [143,144] stated that fatigue cracks will initiate at the sharp intrusions when high-distortion energy is achieved within a crystal area where significant tri-axiality is present. However, present 3D simulations by Déprés et al. have reached only very limited number of cycles (23 cycles) [142–144] and thus further comparison with experimental results will be possible only when more effective computer algorithm allows to extend calculations to appreciable number of loading cycles.

6. Surface relief topography of PSMs and its relation to fatigue crack initiation[12]

The decisive role of surface relief topography in the process of fatigue crack nucleation has been repeatedly demonstrated by electropolishing experiments (for review see e.g. [73]). Thompson et al. [6, 94] for polycrystalline copper and later Basinski et al. [120] for copper single crystals showed that periodical removing of thin surface layer containing extrusions, intrusions and already nucleated cracks by electropolishing leads to a drastic enhancement of

[12] Only transcrystalline crack initiation mode is considered in this section. In addition to this mode PSBs or PSMs can play a role also in crack initiation along grain or twin boundaries, see e.g. [38,76,147,148]. For detail description of different mechanisms proposed for intercrystalline crack initiation mode see e.g. [12,14,15].

fatigue life. Thus a successful model of the surface relief evolution on an originally flat surface due to localized cyclic plastic straining represents the first step to the realistic model of fatigue crack nucleation.

6.1. *Results of experimental observations*

Crack initiation and early crack growth with respect to the surface relief topography were studied mainly for macro-PSMs in copper single crystals using sharp corner polishing technique [14,43–45,73,87,137,149] and section micromilling technique [41,42,75]. It was found that cracks initiate from intrusions everywhere within a protrusion and along macro-PSB-matrix interfaces *A* and *B* as indicated in figure 2(c). In both cases the stage I cracks grow crystallographically along the primary slip plane. A tendency to form deeper cracks preferentially at interfaces *A* and *B* [41,42,44,73,87] (with priority at the side *B* of macro-PSM [41,42,72,87] – see figure 2(c)) has been repeatedly reported. Basinski and Basinski using true-replica technique showed that their depth is not constant along the length, so that a wavy front advances into the crystal [40,45,73].

Some pertinent experimental results concerning the crack initiation were reported also for individual PSMs. In spite of their variability two characteristic forms of extrusion-intrusion morphology shown in figure 2(a) and 2(b) were found not only in copper single crystal [8,12,23,39,71,78,92,109] but also in different f.c.c. [12,20,46,69,70,76,82–86,109, 114,131,150,151] and b.c.c. [30,74,150,152–155] polycrystals. Recent systematic AFM study of evolution of PSMs with respect to the crystallographic orientation of individual grains of 316L steel showed that intrusions arise along ribbon-like extrusions early in fatigue life. Already after 2 000 cycles (4.3% N_f) more than 96% of ribbon-like extrusions are accompanied by at least one parallel intrusion (68% by two intrusions) [20]. In addition to cracks initiated and growing along ribbon-like extrusions, more frequently detected at different stages of fatigue life, the rows of tongue-like cracks, or later shallow surface cracks, have been observed early in fatigue life along PSMs in numerous microcrack initiation studies using replica technique. Anton and Fine [151] and Kim and Fine [152] found crack formation between the hills and valleys of a slip band. At later stage, the cracks started to grow in the interior of the grain. Alternating extrusions and intrusions, and subsequently a shallow crack, were found by Kwon et al. [83] along the PSM in polycrystalline copper.

Direct evidence of crack initiation and early crack growth with regard to the dislocation structure of PSBs and surface topography of PSMs has been obtained very rarely so far [32,47]. Katagiri et al. [32] using ultra HVEM (see table 1) in fatigued polycrystalline

copper revealed cracks nucleating along the PSB-matrix interface at the root of a surface intrusion. They found two kinds of stage I crack routes along the PSBs with ladder structure – in the centre of PSB or along the PSB-matrix boundary. Contrary to stage II cracks, the presence of these cracks running along PSBs caused no appreciable changes in dislocation structure of PSBs. Ahmed et al. [47], using ECCI, studied dislocation structures in the vicinity of stage I and II cracks in copper single crystals prepared by sharp-corner polishing technique (see table 1). Their results indicate that well developed stage I cracks (~ 60 μm in depth) propagate along the centre of PSBs, rather than at PSB-matrix interface. Again, whereas propagation of stage I cracks along PSBs produced no observable changes in local dislocation substructures, the transition to stage II crack growth was associated with deviation from PSB plane and with significant modification of dislocation structure within an extensive crack tip plastic zone [47].

6.2. *Experimental observations of crack initiation versus theoretical models*

All pertinent theoretical models and computational modelling (see sections 5 and 6) of surface relief formation leading to transcrystalline crack initiation are briefly summarised in table 2. In addition to their applicability for the formation of PSMs observed in single crystals or polycrystals, the origin of fatigue crack and the criterion of fatigue crack initiation are also included in this table. It is apparent from this table that except for the models by Mura and co-workers and by Rossenbloom and Laird all of them are applicable for both single crystals and polycrystals. Furthermore, with the exception of the model by Brown and co-workers and EGM-model, intrusions developed at the free surface are considered as an origin of fatigue cracks in all models. Though these models distinguish between intrusion and crack nuclei[13] – see table 2, they do not consider the mechanism of fatigue crack initiation in detail. Another feature striking for many theoretical models is the fact that fatigue crack embryos appear and grow preferentially or exclusively along PSB-matrix interface.

[Insert table 2 about here]

Although both extrusions and intrusions can induce concentration of the stress and strain, intrusions are believed to be more effective stress raiser since the radius of intrusion is

[13] Although there is no consensus on the definition of a just nucleated crack so far, detailed observation of surface relief topography of macro-PSMs in copper single crystals using section micromilling technique by Hunsche and Neumann [42,75] suggests that intrusions and crack nuclei are distinctive different in two aspects: (1) their geometrical shapes are different (vertex angle 30° or 0°, respectively) and (2) intrusion formation does not depend on the environment, whereas crack formation and growth do strongly depend on the environment.

very small and therefore cracks usually start from them. The sharp-corner polishing technique and the section micromilling technique applied to copper single crystals (see table 1) permit estimation of the notch radius to 100 nm. The stress and strain concentration in the tip of an intrusion is thus comparable to that of a crack of the same dimensions. The high stress concentration in the tip of an intrusion gives rise to a local slip-unslip mechanism along primary slip plane. This irreversible slip-unslip mechanism was originally considered by Thompson et al. [6] and Wood [26].

[Insert figure 10 about here]

The more specific model of fatigue crack nucleation taking into account two typical forms of extrusions and intrusions formed within individual PSMs during cycling (see figure 2(a) and 2(b)) and environmentally assisted slip irreversibility has been proposed by Polák and Liškutín [84]. Figure 10(a) shows schematically the environmentally assisted nucleation of surface cracks from a row of intrusions. The semi-elliptical intrusions are nucleated along the PSM and alternate with the extrusions. Material between the neighbouring intrusions is subjected to antiplane shear deformation (mode III). Under this shear deformation mode and environmentally assisted slip irreversibility new surfaces between the intrusions will arise and finally the shallow inclined surface crack will be created. This mechanism can explain why the tongue-like extrusions between two adjacent intrusions are cut by a crack. Figure 10(b) shows schematically the slip-unslip mechanism (mode II) starting from the tip of an intrusion (going parallel along an extrusion at the PSB-matrix interface – see figure 2(b)) under the action of a corrosive environment, which prevents the rewelding of new surfaces. The early phase of a shallow microcrack nucleation from the tip of an intrusion is the result of an irreversible slip along the primary slip plane. In the tensile period a new surface is formed. The complete rewelding of the new surface in the compression phase of a cycle is prevented by the corrosive environment. As it was already mentioned in section 3 the crack advance thus depends appreciably on the aggressiveness of this environment.

Considering the specific dislocation structure of macro-PSBs in the early and later stages of fatigue life the above slip-unslip concept can be also applied to macro-PSMs. In the early stage of fatigue life, when macro-PSB consists of individual ladder-like PSBs separated by thin sheets of the matrix [123], cracks will nucleate everywhere within a protrusion by identical environmentally assisted slip-unslip mechanism shown in figure 10. A set of parallel cracks will arise within a macro-PSM (see figure 2(c)). Later, since the secondary slip is activated, a macro-PSB consists of (misoriented) cell [120,123] or labyrinth [121] structure in

the centre and thin layers of ladder structure are present only close to macro-PSB-matrix interface, cracks will have tendency to grow preferentially along these interfaces.

The tendency to form deeper cracks preferentially at interfaces *A* and *B* between macro-PSB and the matrix (see figure 2(c)) is in agreement with macro-PSB slip behaviour reported repeatedly by Laird and his collaborators [14,24,71,87] and by Basinski et al. [120]. Using optical interferometry they revealed that the strain within the macro-PSBs is not uniformly distributed and local strain greater than the average strain develops at the macro-PSB–matrix interface. The reason for the formation of deeper cracks at side *B* of a macro-PSM contrary to side *A* (see figure 2(c)) is not understood yet. Neumann [41] and Hunsche and Neumann [42] suggest that side *B* may be a preferred crack nucleation site because there are large local lattice rotations (of the order of twenty degrees in copper single crystal [41]) developed during the growth of a protrusion which results in considerable local bending of the primary slip plane. Similar but smaller lattice rotation (about 6 degrees) was reported by Zhai et al. [156] for a macro-PSB in fatigued aluminium single crystals. These authors also claim that such lattice rotation is one of the important factors controlling crack initiation and early propagation.

Preferential site of crack initiation along the PSB-matrix interfaces is explicitly considered only in the model of Brown and co-workers[14] in dependence on the sense of macroscopic internal stress field within an individual PSB (see section 4.1.1). A review of the literature on other pertinent experimental observations at different stages in fatigue life [20,102] shows that there is no general agreement on the question of whether the cracks nucleate at point *A* or at point *B*. Experimental results obtained recently by Man et al. [20] showed that the first intrusions start much more frequently at the PSB-matrix interface denoted *B* (compare figures 2(b) and 3) which is in agreement with the model by Brown and co-workers provided that macroscopic tensile internal stress is present in a PSB lamella. Nevertheless, there are also another two arguments which prefer *B* side for crack initiation. Firstly, the notch developed at side *B* is sharper (i.e. it represents more effective stress and strain raiser) – see figure 5. This geometrical consideration is in agreement with the EGM model [18,38] and with the numerical simulations by Repetto and Ortiz [138]. Secondly, Sauzay and Gilormini [157] used the finite element method to estimate distribution of the plastic slip range within a surface PSB with various aspect ratios, cyclically loaded under an

[14] Although Brown and co-workers in their model do not distinguish specifically between individual PSBs and macro-PSBs, their model can be applied also to macro-PSBs, reflecting their specific dislocation structure observed in the early and later stages of fatigue life (see above) [103].

alternating uniaxial remote stress. The largest slip was always obtained at the surface along the PSB-matrix interface *B* (see figure 2(b)) [157].

7. Concluding remarks

The surface relief formation leading to crack initiation in cyclically strained materials is an important subject in the field of fatigue of materials. Considerable progress in the knowledge on surface relief topography using various experimental techniques contributed to the elucidation of the mechanisms leading to transcrystalline fatigue crack initiation.

Nevertheless, the detailed review of the theoretical models and computational simulations of surface relief evolution leading to fatigue crack initiation presented above demonstrates only partial understanding of the subject. All the models were developed under simplified conditions and have been verified only partly by experimental studies. The future development in this field must encompass interdisciplinary approach leading to exact quantitative description of surface relief evolution and fatigue crack initiation.

Understanding of the fatigue crack initiation represents one of the most difficult tasks in the study of basic fatigue phenomena. The success is closely related to the level of experimental techniques. Considerable variability in the surface relief topography of PSMs is an important factor. Fong [158] pointed out aptly that direct observations are the essential ingredients for discovering fundamental mechanisms (not only) in fatigue. We still do not know enough about the magnitude and nature of the internal stresses within individual PSBs, how they build up during cycling, about the slip activity of individual PSBs, about the shape and geometry of individual PSMs and their relation to dislocation structure of PSB and to the fatigue crack initiation site, about the kinetics of simultaneous growth of extrusions and intrusions at depressed and elevated temperatures, and about the role of lattice defects (mainly point defects) in the surface relief formation and fatigue crack initiation. Such information will be invaluable for further verification and/or modification of the existing models of fatigue crack initiation and for comparison with the results of expanding computer modelling. It will lead to the formulation of a more complete quantitative theory of the early fatigue damage. AFM, SEM-FEG equipped by FIB, ECCI and EBSD technique, positron lifetime measurements with high spatial resolution, computed x-ray micro-tomography and other developing modern experimental techniques with high resolution can be tools for obtaining such information in a quantitative form.

Acknowledgements

The authors are grateful for several useful discussions to Prof. L. M. Brown (the model of his group) and to Dr. E. Hieckmann (formerly Thiele) (internal stresses within PSBs). They are also indebted to an anonymous referee for his critical and stimulating comments on the manuscript. The support of the present work by the grants No. 106/06/1096 and No. 101/07/1500 of the Grant Agency of the Czech Republic and by the research project No. AV0Z 20410507 and the grant No. 1QS200410502 of the Academy of Sciences of the Czech Republic is acknowledged.

References

[1] J.A. Ewing and J.C.W. Humfrey, Phil. Trans. Roy. Soc. (London) A 200 (1903) p. 241.

[2] P.J.E. Forsyth, Nature 171 (1953) p. 172.

[3] D. Hull, J. Inst. Metals 84 (1955–56) p. 527.

[4] A.H. Cottrell and D. Hull, Proc. Roy. Soc. A 242 (1957) p. 211.

[5] P.J.E. Forsyth, Proc. Roy. Soc. A 242 (1957) p. 198.

[6] N. Thompson, N.J. Wadsworth, and N. Louat, Phil. Mag. 1 (1956) p. 113.

[7] E.E. Laufer and W.N. Roberts, Phil. Mag. 10 (1964) p. 883.

[8] E.E. Laufer and W.N. Roberts, Phil. Mag. 14 (1966) p. 65.

[9] P. Lukáš, M. Klesnil and J. Krejčí, Phys. Stat. Sol. 27 (1968) p. 545.

[10] J.D. Atkinson, L.M. Brown, R. Kwadjo et al., *The structure of persistent slip bands and the fatigue strength of metals*, in *The Microstructure and Design of Alloys*, *Proceedings of the Third International Conference on the Strength of Metals and Alloys (ICSMA 3)*, Vol. 1, Cambridge, England, 1973, paper. No. 82, pp. 402–406.

[11] C. Laird, P. Charsley and H. Mughrabi, Mater. Sci. Eng. 81 (1986) p. 433.

[12] J. Polák, *Cyclic deformation, crack initiation, and low-cycle fatigue*, in *Comprehensive Structural Integrity*, Vol. 4, I. Milne, R.O. Ritchie, and B. Karihallo, eds., Elsevier, Amsterdam, 2003, pp. 1–39.

[13] P. Lukáš and L. Kunz, Phil. Mag. 84 (2004) p. 317.

[14] C. Laird, *Fatigue*, in *Physical Metallurgy*, R.W. Cahn and P. Haasen, eds., 4th ed., Vol. 3, Chapter 27, Elsevier Science, Amsterdam, 1996, pp. 2293–2397.

[15] S. Suresh, *Fatigue of Materials*, 2nd ed., Cambridge University Press, Cambridge, 1998.

[16] P. Lukáš, *Fatigue crack initiation mechanisms*, in *Encyclopedia of Materials: Science and Technology*, Vol. 3, K.H.J. Buschow, R.W. Cahn, M.C. Flemings et al., eds., Elsevier Science, Oxford, 2001, pp. 2884–2894.

[17] H. Mughrabi, *Cyclic strain localization in fatigued metals*, in *Physical Aspects of Fracture*, NATO Science Series, Vol. II/32, E. Bouchaud, D. Jeulin, C. Prioul and S. Roux, eds., Kluwer Academic Publishers, Dordrecht, 2001, pp. 271–281.

[18] U. Essmann, U. Gösele and H. Mughrabi, Phil. Mag. A 44 (1981) p. 405.

[19] J.G. Antonopoulos, L.M. Brown and A.T. Winter, Phil. Mag. 34 (1976) p. 549.

[20] J. Man, P. Klapetek, O. Man et al., Phil. Mag. (2008), submitted for publication.

[21] D.L. Davidson, *Techniques for investigating fatigue*, in *Proceedings of the Sixth International Fatigue Congress (FATIGUE '96)*, Vol. III, G. Lütjering and H. Nowack, eds., Pergamon, Oxford, 1996, pp. 1925–1935.

[22] P.J.E. Forsyth, J. Inst. Metals 82 (1953–54) p. 449.

[23] P. Neumann, Z. Metallk. 58 (1967) p. 780.

[24] J.M. Finney and C. Laird, Phil. Mag. 31 (1975) p. 339.

[25] S.L. Ogin and L.M. Brown, *A preliminary study of persistent slip bands in AgCl*, in *Dislocation Modelling of Physical Systems*, M.F. Ashby, R. Bullough, C.S. Hartley and J.P. Hirth, eds., Pergamon Press, Oxford, 1981, pp. 579–586.

[26] W.A. Wood, Phil. Mag. 3 (1958) p. 692.

[27] D.H. Avery, G.A. Miller and W.A. Backofen, Acta Metall. 9 (1961) p. 892.

[28] W.D. Dover and W.J.D. Jones, Brit. J. Appl. Phys. 18 (1967) p. 1257.

[29] A. Ueno and H. Kishimoto, *Development of in-situ observation fatigue testing systems and their application*, in *Fatigue '99*, *Proceedings of the Seventh International Fatigue Congress*, Vol. 4/4, X.R. Wu and Z.G. Wang, eds., Higher Education Press/EMAS, Beijing/West Midlands, UK, 1999, pp. 2795–2800.

[30] M. Hempel, *Metallographic observations on the fatigue of steels*, in *Proceedings of the International Conference on Fatigue of Metals*, The Institution of Mechanical Engineers, London, 1956, pp. 543–547.

[31] D. Hull, J. Inst. Metals 86 (1957–58) p. 425.

[32] K. Katagiri, A. Omura, K. Koyanagi et al., Met. Trans. 8A (1977) p. 1769.

[33] I.G. Greenfield, Acta Metall. 19 (1971) p. 857.

[34] A.W. Thompson, Acta Metall. 20 (1972) p. 1085.

[35] A.T. Winter, Phil. Mag. 30 (1974) p. 719.

[36] W. Kromp, B. Weiss and R. Stickler, Metall. Trans. 4 (1973) p. 1167.

[37] R. Wang, B. Bauer and H. Mughrabi, Z. Metallk. 73 (1982) p. 30.

[38] H. Mughrabi, R. Wang, K. Differt et al., *Fatigue crack initiation by cyclic slip irreversibilities in high-cycle fatigue*, in *Fatigue Mechanisms: Advances in Quantitative Measurement of Physical Damage*, ASTM STP 811, J. Lankford, D.L. Davidson, W.L. Morris and R.P. Wei, eds., American Society for Testing and Materials, Philadelphia, 1983, pp. 5–45.

[39] J. Polák, T. Lepistö and P. Kettunen, Mater. Sci. Eng. 74 (1985) p. 85.

[40] Z.S. Basinski and S.J. Basinski, Acta metall. 33 (1985) p. 1307

[41] P. Neumann, *Fatigue*, in *Physical Metallurgy*, 3rd. ed., Part 2, chapter 24, R. W. Cahn and P. Haasen, eds., Elsevier Science, Amsterdam, 1983, pp. 1553–1594.

[42] A. Hunsche and P. Neumann, Acta metall. 34 (1986) p. 207.

[43] Z.S. Basinski and S.J. Basinski, Scripta metall. 18 (1984) p. 851.

[44] Z.S. Basinski and S.J. Basinski, Acta metall. 37 (1989) p. 3263.

[45] Z.S. Basinski and S.J. Basinski, Acta metall. 33 (1985) p. 1319.

[46] J. Polák and T. Kruml, *Topography of the crack nuclei at the emerging persistent slip band in austenitic 316L steel*, in *Low Cycle Fatigue and Elasto-Plastic Behaviour of Materials*, K.-T. Rie and P. D. Portella, eds., Elsevier Science, Oxford, 1998, pp. 559–564.

[47] J. Ahmed, A.J. Wilkinson and S.G. Roberts, Phil. Mag. A 81 (2001) p. 1473.

[48] O. Kraft, P. Wellner, M. Hommel et al., Z. Metallk. 93 (2002) p. 392.

[49] Y. Motoyashiki, A. Brückner-Foit and A. Sugeta, Fatigue Fract. Engng. Mater. Struct. 29 (2007) p. 556.

[50] J. Polák, J. Man, T. Vystavěl et al., Key Eng. Mater. 345–346 (2007) p. 379.

[51] K. Gall, G. Biallas, H.J. Maier et al., Metall. Mater. Trans. A 35 (2004) p. 321.

[52] G. Biallas and H.J. Maier, Int. J. Fatigue 29 (2007) p. 1413.

[53] A. Weidner, R. Beyer, C. Blochwitz et al., Mater. Sci. Eng. A 435–436 (2006) p. 540.

[54] A. Weidner, C. Blochwitz, W. Skrotzki et al., Mater. Sci. Eng. A 479 (2008) p. 181.

[55] W.J. Baxter, *What are the kinetics of slipband extrusion?*, in *Basic Questions in Fatigue: Volume I*, ASTM STP 924, J.T. Fong and R.J. Fields, eds., American Society for Testing and Materials, Philadelphia, 1988, pp. 67–80.

[56] W.J. Baxter and T.R. McKinney, Metall. Trans. A 19 (1988) p. 83.

[57] T.-G. Zhai, S. Lin and J.-M. Xiao, Acta metal. mater. 38 (1990) p. 1687.

[58] T. Zhai, J.W. Martin and G.A.D. Briggs, Acta metal. mater. 43 (1995) p. 3813.

[60] G. Venkataraman, T.S. Sriram, M.E. Fine et al., Scripta Metall. Mater. 24 (1990) p. 273.

[61] T.S. Sriram, M.E. Fine and Y.W. Chung, Scripta Metall. Mater. 24 (1990) p. 279.

[62] J.C. Grosskreutz, C.Q. Bowles and A.A. Wahab, J. Mater. Sci. 27 (1992) p. 5756.

[63] H. Ishii, S. Miyazu, K. Nagura et al., Trans. Japan Soc. Mech. Eng. A 59 (1993) p. 3014.

[64] S.E. Harvey, P.G. Marsh and W.W. Gerberich, Acta metall. mater. 42 (1994) p. 3493.

[65] Y. Nakai, S. Fukuhara and K. Ohnishi, Int. J. Fatigue 19 (1997) p. S223.

[66] J. Man, K. Obrtlík, F. Lopour et al., *AFM quantitative evaluation of surface relief topography in fatigued 316L stainless steel*, in *Fatigue '99*, *Proceedings of the Seventh International Fatigue Congress*, Vol. 1/4, X.R. Wu and Z.G. Wang, eds., Higher Education Press/EMAS, Beijing/West Midlands, UK, 1999, pp. 157–162.

[67] L. Sabatier, P. Villechaise and J.C. Girard, J. Phys. IV France 10 (2000) p. Pr6-197.

[68] Y. Nakai, K. Ohnishi and T. Kusukawa, *Observations of fatigue slip-bands and stage I crack-initiation process in α-brass using scanning atomic-force microscopy*, in *Small Fatigue Cracks: Mechanics, Mechanisms and Applications*, K.S. Ravichandran, R.O. Ritchie and Y. Murakami, eds., Elsevier Science Ltd., Oxford, 1999, pp. 343–352.

[69] J. Polák, J. Man and K. Obrtlík, Int. J. Fatigue 25 (2003) p. 1027.

[70] J. Polák, J. Man, K. Obrtlík et al., Z. Metallk. 94 (2003) p. 1327.

[71] D.E. Witmer, G.C. Farrington and C. Laird, Acta metall. 35 (1987) p. 1895.

[72] J. Dönch and P. Haasen, Z. Metallk. 62 (1971) p. 780.

[73] Z.S. Basinski and S.J. Basinski, Prog. Mater. Sci. 36 (1992) p. 89.

[74] J. Man, M. Petrenec, K. Obrtlík et al., Acta Mater. 52 (2004) p. 5551.

[75] A. Hunsche and P. Neumann, *Crack nucleation in persistent slip bands*, in *Basic Questions in Fatigue: Volume I*, ASTM STP 924, J.T. Fong and R.J. Fields, eds., American Society for Testing and Materials, Philadelphia, 1988, pp. 26–38.

[76] P. Neumann and A. Tönnessen, *Cyclic deformation and crack initiation*, in *Fatigue '87, Proceedings of the Third International Conference on Fatigue and Fatigue Thresholds*, Vol. 1, R.O. Ritchie and E.A. Starke, Jr., eds., EMAS, West Midlands, UK, 1987, pp. 3–22.

[77] P. Neumann, *Analytical solution for the incompatibility stresses at twin boundaries in cubic crystals*, in *Fatigue '99, Proceedings of the Seventh International Fatigue Congress*, Vol. 1/4, X.R. Wu and Z.G. Wang, eds., Higher Education Press/EMAS, Beijing/West Midlands, UK, 1999, pp. 107–114.

[78] H. Mughrabi, M. Bayerlein, and R. Wang, *Direct measurement of the rate of extrusion growth in fatigued copper mono- and polycrystals*, in *Proceedings of the Ninth International Conference on Strength of Metals and Alloys (ICSMA 9)*, Vol. 2, D.G. Brandon, R. Chaim, and A. Rosen, eds., Freund Publ. Comp., London, 1991, pp. 879–886.

[79] P. Villechaise, L. Sabatier and J.C. Girard, Mater. Sci. Eng. A 323 (2002) p. 377.

[80] J. Man, K. Obrtlík, C. Blochwitz et al., Acta Mater. 50 (2002) p. 3767.

[81] H. Mughrabi, *Dislocations in fatigue*, in *Dislocations and Properties of Real Materials*, Book No. 323, The Institute of Metals, London, 1985, pp. 244–262.

[82] J. Man, K. Obrtlík and J. Polák, Mater. Sci. Eng. A 351 (2003) p. 123.

[83] I.B. Kwon, M.E. Fine and J. Weertman, Acta metall. 37 (1989) p. 2927.

[84] J. Polák and P. Liškutín, Fatigue Fract. Engng Mater. Struct. 13 (1990) p. 119.

[85] M. Bayerlein and H. Mughrabi, Acta metall. mater. 39 (1991) p. 1645.

[86] G.-H. Kim, I.-B. Kwon and M.E. Fine, Mater. Sci. Eng. A 142 (1991) p. 177.

[87] B.-T. Ma and C. Laird, Acta metall. 37 (1989) p. 325.

[88] R. Wang, H. Mughrabi, S. McGovern et al., Mater. Sci. Eng. 65 (1984) p. 219.

[89] K. Obrtlík, J. Man and J. Polák, Mater. Sci. Eng. A 234–236 (1997) p. 727.

[90] J. Man, K. Obrtlík and J. Polák, Metallic Mater. 38 (2000) p. 339.

[91] K. Mecke and C. Blochwitz, phys. stat. sol. (a) 61 (1980) p. K5.

[92] I.B. Kwon, M.E. Fine and J. Weertman, Acta metall. 37 (1989) p. 2937.

[93] P.G. Partridge, Acta metall. 13 (1965) p. 517.

[94] N. Thompson and N.J. Wadsworth, Adv. Phys. 7 (1958) p. 72.

[95] A.J. Kennedy, *Processes of Creep and Fatigue in Metals*, Oliver & Boyd, Edinburgh and London, 1962, pp. 331–346.

[96] J.R. Low, Jr., Prog. Mater. Sci. 12 (1963) p. 3.

[97] C. Laird and D.J. Duquette, *Mechanisms of fatigue crack nucleation*, in *Corrosion Fatigue: Chemistry, Mechanics and Microstructure*, Vol. NACE-2, O.F. Devereux, A.J. McEvily and R.W. Staehle, eds., National Association of Corrosion Engineers, Houston, 1972, pp. 88–117.

[98] S. Kocanda, *Fatigue Failure of Metals*, Sijthoff and Nordhoff, Warsaw, 1978, pp. 67–77.

[99] T.H. Lin and S.R. Lin, *Micromechanics theory of fatigue crack initiation applied to time-dependent fatigue*, in *Fatigue Mechanisms*, ASTM STP 675, J.T. Fong, ed., American Society for Testing and Materials, Philadelphia, 1979, pp. 707–728.

[100] L.M. Brown, Metal Sci. 11 (1977) p. 315.

[101] L.M. Brown, *Dislocations and the fatigue strength of metals*, in *Dislocation Modelling of Physical Systems*, M.F. Ashby, R. Bullough, C.S. Hartley and J.P. Hirth, eds., Pergamon Press, Oxford, 1981, pp. 51–68.

[102] L.M. Brown and S.L. Ogin, *Role of internal stresses in the nucleation of fatigue cracks*, in *Fundamentals of Deformation and Fracture*, B.A. Bilby, K.J. Miller and J.R. Willis, eds., Cambridge University Press, Cambridge, 1985, pp. 501–528.

[103] L.M. Brown, *Deformation mechanisms leading to the initiation and slow growth of fatigue cracks*, in *Modelling of Material Behavior and Design*, J.D. Embury and A.W. Thompson, eds., TMS-AIME, Warrendale, PA, 1990, pp. 175–198.

[104] L.M. Brown and F.R.N. Nabarro, Phil. Mag. 84 (2004) p. 441.

[105] C. Buque, W. Tirschler and C. Holste, Mater. Sci. Eng. A 215 (1996) p. 168.

[106] L.M. Brown, private communication (2004).

[107] L. Cretegny and A. Saxena, Acta Mater. 49 (2001) p. 3755.

[108] K. Differt, U. Essmann and H. Mughrabi, Phil. Mag. A 54 (1986) p. 237.

[109] J. Polák, Mater. Sci. Eng. 92 (1987) p. 71.

[110] J. Polák, Mater. Sci. Eng. A 468–470 (2007) p. 33.

[111] J. Polák, M. Sauzay, Mater. Sci. Eng. A 500 (2009) p. 122.

[112] J. Polák, Solid State Phenom. (Dislocations 93) 35-36 (1994) p. 405.

[113] J. Polák, Mater. Sci. Eng. 89 (1987) p. 35.

[114] L.M. Hsiung and N.S. Stoloff, Acta metall. Mater. 38 (1990) p. 1191.

[115] T.H. Lin and Y.M. Ito, Proc. N. A. S. 62 (1969) p. 631.

[116] T.H. Lin, S.R. Lin and X.Q. Wu, Phil. Mag. A 59 (1989) p. 1263.

[117] T.H. Lin, Adv. Appl. Mech. 29 (1992) p. 1.

[118] T.H. Lin, N.G. Liang, K.F.F. Wong et al., Phil. Mag. A 80 (2000) p. 1829.

[119] W.A. Wood and A.M. Bendler, Trans. Metall. Soc. AIME 224 (1962) p. 180.

[120] Z.S. Basinski, R. Pascual and S.J. Basinski, Acta metall. 31 (1983) p. 591.

[121] P. Ackermann, L.P. Kubin, J. Lepinoux et al., Acta metall. 32 (1984) p. 715.

[122] R. Wang and H. Mughrabi, Mater. Sci. Eng. 63 (1984) p. 147.

[123] J. Polák and K. Obrtlík, *Surface relief and dislocation structure in fatigued copper single crystals*, in *Proceedings of the 8th International Conference on the Strength of Metals and Alloys (ICSMA 8)*, Vol. 1/2, P.O. Kettunen, T.K. Lepistö and M.E. Lehtonen, eds., Pergamon Press, Oxford, 1988, pp. 761–766.

[124] T. Zhai, J.W. Martin and G.A.D. Briggs, Acta mater. 44 (1996) p. 3489.

[125] K. Tanaka and T. Mura, J. Appl. Mech. 48 (1981) p. 97.

[126] G. Venkataraman, Y.W. Chung, Y. Nakasone et al., Acta metall. mater. 38 (1990) p. 31.

[127] G. Venkataraman, Y.W. Chung and T. Mura, Acta metall. mater. 39 (1991) p. 2621.

[128] K.S. Chan, Metall. Mater. Trans. A 34 (2003) p. 43.

[129] G. Venkataraman, Y.W. Chung and T. Mura, Acta metall. mater. 39 (1991) p. 2631.

[130] Z.S. Basinski and S.J. Basinski, Scripta metall. mater. 26 (1992) p. 1505.

[131] J.I. Dickson, J.-P. Baïlon, J. Xia et al., *Extrusion-intrusion formation in Cu and 70Cu-30Zn*, in *Proceedings of the Fifth International Conference on Fatigue and Fatigue Thresholds (FATIGUE `93)*, Vol. III, J.-P. Baïlon and J.I. Dickson, eds., EMAS, West Midlands, UK, 1993, pp. 1883–1892.

[132] P. Neumann, H. Fuhlrott and H. Vehoff, *Experiments concerning brittle, ductile, and environmentally controlled fatigue crack growth*, in *Fatigue Mechanisms*, ASTM STP 675, J.T. Fong, ed., American Society for Testing and Materials, Philadelphia, 1979, pp. 371–395.

[133] U. Essmann, Phil. Mag. A 45 (1982) p. 171.

[134] S.N. Rosenbloom and C. Laird, Acta metall. mater. 41 (1993) p. 3473.

[135] A.N. May, Nature 185 (1960) p. 303.

[136] A.N. May, Nature 185 (1960) p. 573.

[137] B.-T. Ma and C. Laird, Acta metall. 37 (1989) p. 337.

[138] E.A. Repetto and M. Ortiz, Acta mater. 45 (1997) p. 2577.

[139] A.C. Damask and G.J. Dienes, *Point Defects in Metals*, Gordon and Breach, New York, 1963.

[140] S. Brinckmann and E. Van der Giessen, *Stress concentration at the surface of fatigued materials: a discrete dislocation dynamics study*, in *Advances in Computational and Experimental Engineering and Sciences (ICCES03)*, S. N. Atluri, D.E. Beskos and D. Polyzos, eds., 2003.

[141] S. Brinckmann and E. Van der Giessen, Mater. Sci. Eng. A 387–389 (2004) p. 461.

[142] C. Déprés, C.F. Robertson and M.C. Fivel, Phil. Mag. 84 (2004) p. 2257.

[143] C. Déprés, C.F. Robertson and M.C. Fivel, Mater. Sci. Eng. A 387–389 (2004) p. 288.

[144] C. Déprés, C.F. Robertson and M.C. Fivel, Phil. Mag. 86 (2006) p. 79.

[145] M.V. Glazov and C. Laird, Acta metall. mater. 43 (1993) p. 2849.

[146] C. Holste, Phil. Mag. 84 (2004) pp. 299.

[147] G. Dörr and C. Blochwitz, Cryst. Res. Technol. 22 (1987) p. 113.

[148] W. Liu, M. Bayerlein, H. Mughrabi et al., Acta metall. mater. 40 (1992) p. 1763.

[149] B.-T. Ma and C. Laird, Acta metall. mater. 38 (1990) p. 1693.

[150] J. Polák, K. Obrtlík and P. Liškutín, *Mechanisms of fatigue crack initiation*, in *Basic Mechanisms in Fatigue of Metals*, P. Lukáš and J. Polák, eds., Academia/Elsevier, Prague/Amsterdam, 1988, pp. 101–109.

[151] D.L. Anton and M.E. Fine, Mater. Sci. Eng. 58 (1983) p. 135.

[152] Y.H. Kim and M.E. Fine, Metall. Trans. A 13A (1982) p. 59.

[153] W.J. Lee, Y.W. Chung and M.E. Fine, Metall. Trans. A 19A (1988) p. 337.

[154] N.J. Roven and E. Nes, Acta metall. mater. 39 (1991) p. 1719.

[155] L.C. Rolim Lopes and J. Charlier, Mater. Sci. Eng. A 169 (1993) p. 67.

[156] T. Zhai, J.W. Martin, G.A.D. Briggs et al., Acta metal. mater. 44 (1996) p. 3477.

[157] M. Sauzay and P. Gilormini, Theor. Appl. Fract. Mech. 38 (2002) p. 53.

[158] J.T. Fong, *Direct observations – the essential ingredients for discovering fundamental mechanisms of fatigue*, in *Fatigue Mechanisms*, ASTM STP 675, J.T. Fong, ed., American Society for Testing and Materials, Philadelphia, 1979, pp. 287–291.

Figure captions

Figure 1. Section through the grain showing surface profile of mature PSM formed at the side where PSB intersects free surface. The dislocation distributions in PSB with so-called ladder structure embedded in the matrix with vein structure are indicated schematically according to Essmann et al. [18]. Dipolar nature of the walls in PSB is highlighted in agreement with Antonopoulos et al. [19].

Figure 2. Schematic diagram of three characteristic forms of mature PSM morphology in fatigued f.c.c. metals. (a) (Quasi-) periodic alternations of tongue-like extrusions and intrusions along PSB surface trace. (b) Ribbon-like extrusion accompanied by two (or by one) parallel intrusions at PSB-matrix interface. (c) Surface relief of a macro-PSB traversing typically the whole cross-section of single crystal with indicated cracks initiated both within macro-PSM and at macro-PSB/matrix interface. Labelling of PSB/matrix interfaces *A* and *B* is in agreement with model by Brown and co-workers and with EGM model.

Figure 3. Model of fatigue crack initiation by Brown and co-workers (schematically). (a) General sketch of PSB with (static) extrusions at its both ends to model elastic tensile macroscopic internal stresses within PSB. Surface cracks (decohesions) going along PSB-matrix interfaces and opened due to stress singularities at the intersections of PSB with the surface are indicated. (b) Detail of PSB showing the dislocation walls composed of vacancy dipoles and the larger, imaginary dipoles which help in visualizing the internal stress within PSB. (c) Surface stresses σ_{yy} at the intersection of PSB with the free surface. The stress is tensile at the point *B* and compressive at the point *A* if the dislocations have the sign shown. Vertical axis scales with PSB width *w*. After [19,102,106]. *(Figure 3(c) reprinted from [102] with permission from Cambridge University Press)*

Figure 4. Model of microcrack initiation in a PSB on the side surface containing Burgers vector by Zhai et al. (schematically). (a) A dipolar dislocation wall in the PSB is under a resulting internal tensile stress mainly caused by massive irreversible slip carried by screw dislocations in the surface region. (b) A microcrack initiation from the dislocation wall in the PSB due to the collapse of the wall under the joint action of the internal tensile stress $\sigma_1 + \sigma_2$ and the applied stress. (c) Possible formation of a microvoid due to only a partial collapse of the wall provided the internal tensile stress $\sigma_1 + \sigma_2$ is not uniform along the wall. After [57,58]. *(Reprinted with permission from Elsevier)*

Figure 5. Model by Essmann, Gösele and Mughrabi (EGM-model) of PSB surface profile formation (schematically). (a) Accumulation of PSB-matrix interface dislocations. (b) Rapid formation of static extrusion after emergence of interface dislocations. (c) Slow roughening of the profile of the static extrusion by random slip with indicated two types of the stress raisers considered by EGM for fatigue crack nucleation. **b** – Burgers vector, M – matrix, PSB – persistent slip band, N – number of cycles, $\gamma_{\mathrm{pl,cum}}$ – cumulative plastic shear strain. After [18,81]. *(Adapted from [81]. Copyright © 1985 by The Institute of Metals, London. Reprinted by permission from The Institute of Materials, Minerals and Mining)*

Figure 6. Polák's model of surface relief formation for an individual PSB. (a) Schematic section through a crystal containing PSB and matrix in a plane $x = 0$ and quasi-stable vacancy concentration profiles within PSB (section $A - A'$) and in a plane perpendicular to PSB (section $B - B'$) in constant frequency cycling. Vacancy fluxes within the PSB and out of the PSB are indicated by arrows. (b) Relation (schematic) between the dislocation structure of a PSB and adjacent PSM when the point defects migrate within the band. (c) Surface profile (schematic) of a PSM when point defects migrate from the band to the matrix. *(Reprinted from [109] with permission from Elsevier)*

Figure 7. The micromechanical model of extrusion and intrusion formation suggested by Lin and his associates. (a) PSB in most favourably oriented grain at the free surface of a polycrystal. The slip plane and the slip direction of the most favourable slip system form an angle of 45° with the specimen axis. (b) Extrusion or (c) intrusion formed at a free surface with the indicated signs in the initial stress field in slices P and Q. After [99,118]. *(Figure 6(b) and 6(c) reprinted from [99] with permission from ASTM International)*

Figure 8. Model by Tanaka and Mura of surface relief formation and fatigue crack initiation in a PSB. (a) Schema of plate-like layers (PSBs) with accumulated dislocation pileups at the grain boundary in most favourably oriented grain and the formation of extrusion, intrusion or extrusion-intrusion pair shown in the section perpendicular to the specimen surface. The dislocation pileups on layers I and II are under tension and compression respectively. (b) Crack initiation from vacancy dipoles or extrusion. (c) Crack initiation from intrusion. *(Taken from [125]. Reprinted by permission of ASME)*

Figure 9. The crack closure-fracture surface rubbing (CCFSR) mechanism for formation of thin extrusions in the presence of a pre-existing small crack in a single crystal suggested by Dickson et al. [131] (schematically). (a) During the compression portion of the load-

decreasing half cycle, the extrusion is produced by a rubbing/burring process on the crack face which subtends an obtuse angle with the specimen surface. The fracture surface rubbing also tends to push the extrusions away from the crack. (b) During the load-increasing portion of the stress cycle, an extrusion can form on the other face, if there is sufficient local crack closure to produce the required fracture surface rubbing. (c) The net effect is that more numerous and larger extrusions are formed on the crack faces subtending an obtuse angle with the specimen surface. *(This figure originally appeared in [131], published by EMAS Publishing in 1993, ISBN: 0–947817–60–3 and is reproduced with their permission – www.emas.co.uk)*

Figure 10. (a) Mechanism of crack nucleation from a row of intrusions quasi-periodically alternating with tongue-like extrusions. (b) Environmentally assisted slip-unslip mechanism leading to crack growth from an intrusion parallel to ribbon-like extrusion (not shown in figure) along the PSB-matrix interface. *(After figure 10 in [84]. Reprinted by permission of Blackwell Publishing)*

Table 1. Development of microscopic techniques used for the study of surface relief of PSMs and fatigue crack initiation.

Microscopy	Specific technique	Summary appraisal of technique
Optical microscopy (OM)	**Specimen surface observation** *Ewing and Humfrey (1903)* [1], *Forsyth (1953)* [2]	Basic simple technique for quick pre-inspection and documentation of specimen surface or plastic replica. Polarised light and Nomarski (differential) interference contrast are very suitable for visualization of very fine surface slip markings at the start of cycling however without possibility of quantitative height measurements.
	Interferometry *Forsyth (1953-54)* [22], *Neumann (1967)* [23], *Finney and Laird (1975)* [24]	Height measurements of protrusions and measurement of slip steps generated in one quarter- or half-cycle after electropolishing. Due to low lateral resolution it is applicable only to macro-PSMs observed in single crystals.
	Surface and stress birefringence observation of optically transparent AgCl ductile ionic crystals *Forsyth (1957)* [5], *Ogin and Brown (1981)* [25]	Observation of the underside of surface and detection of intrusions in AgCl single and polycrystals by transmitted light. Visualization of macroscopic internal stresses associated with PSBs using birefringence observations in AgCl single crystals.
	Taper-sectioning technique‡§ *Wood (1958)* [26], *Avery, Miller and Backofen (1961)* [27]	Height measurements of surface relief. The technique can easily produce inherent artefacts in the observed profiles of extrusions and intrusions.
	Successive sectioning technique‡ *Dover and Jones (1967)* [28]	One of the techniques (also with conjunction with SEM) exploited for the determination of the 3D form of the shape of initial fatigue cracks.
	***In-situ* specimen surface observation by confocal scanning laser microscopy (CSLM)** *Ueno and Kishimoto (1999)* [29]	Optical sections of surface profiles of PSMs (as well as crack front) for 3D reconstruction. High sensitivity for height measurements (extrusion height or intrusion depth via plastic replica), much lower lateral resolution is insufficient for detailed observation of individual PSMs in polycrystals.
Transmission electron microscopy (TEM)	**Shadowed aluminium and two-stage carbon replicas** *Hull (1955-56)* [3], *Hempel (1956)* [30], *Cottrel and Hull (1957)* [4], *Hull (1957-58)* [31]	Imaging of fine details of surface topography within individual PSMs (depending on the replication procedure positive or negative (inverse) image of the specimen surface can be obtained); possibility of semi-quantitative assessment of growth of intrusion or initiated cracks (out-of-plane measurements) in shadowed plastic-carbon replicas. Plastic replica taken from micro-section reveals the connection of surface relief and crack initiation.
	Plastic replica taken from longitudinal micro-section after electroplating *Hempel (1956)* [30]	
	Surface foils after electrodeposition‡ *Lukáš, Klesnil and Krejčí (1968)* [9]	Experimentally difficult technique enabling simultaneous observation of surface relief profiles and associated dislocation substructures.
	Ultra HVEM (high voltage electron microscopy) of surface foils after electrodeposition‡ *Katagiri et al. (1976)* [32]	
Scanning electron microscopy (SEM)	**Specimen surface observation** *Greenfield (1971)* [33], *Thompson (1972)* [34], *Winter (1974)* [35]	Standard technique for qualitative study of topography and surface density (frequency of occurrence) of PSMs; quantitative assessment of PSM topography and its evolution is possible only in conjunction with some of specific techniques (see below).
	***In-situ* specimen surface observation** *Kromp, Weiss and Stickler (1973)* [36]	The technique used for the study of initiated short crack (near-crack-tip slip behaviour, crack opening displacement, crack interactions). Vacuum environment in SEM chamber can represent limitation for some materials.
	Contamination line technique *Wang, Bauer and Mughrabi (1982)* [37], *Mughrabi et al. (1983)* [38]	Determination of the shape and the height of young extrusions in selected sections; the deep parts of PSM-profiles (intrusions) are usually not accessible. It is difficult to apply to all materials (in some cases it needs deposition of gold layer on the specimen surface).

Scanning electron microscopy (SEM) *(cont.)*	**Direct relief-imaging at the edge of the specimen by viewing from the side**§ *Wang, Bauer and Mughrabi (1982)* [37], *Mughrabi et al. (1983)* [38]	Simple and direct method to obtain the outer contours of PSM-profiles (i.e. only extrusions); ideally suited for single crystals oriented for single slip; in polycrystals the technique is limited to coarse-grained materials. To avoid complicated projection effects it needs precise adjustment.
	Viewing surface and/or replica photographs using stereo pairs and quantitative stereometry *Wang, Bauer and Mughrabi (1982)* [37], *Polák, Lepistö and Kettunen (1985)* [39], *Basinski and Basinski (1985)* [40]	Former technique used for 3D visualization of surface relief and for easier identification of cracks or intrusions within PSMs on the specimen surface. 3D reconstruction from stereo pairs providing PSM profiles in quantitative form. It is time-consuming.
	Section micromilling technique‡§ *Neumann (1983)* [41], *Hunsche and Neumann (1986)* [42]	Precise sections perpendicular to the surface (without any deformation of surface details) at predetermined positions with accuracy of a few μm; quantitative study of PSM-profiles and initiated fatigue cracks. The technique is hardly applicable to systematic study in polycrystals.
	Sharp-corner polishing technique§ *Basinski and Basinski (1984)* [43] (detailed description of the technique was published later [44])	Experimentally difficult technique; simultaneous examination of the specimen surface and quantitative study of the evolution of PSM profiles and the initiation and growth of fatigue cracks during fatigue life at the sharp edge of polished specimens. It is applicable only for single crystals and not for polycrystals.
	Lacomit true-replica technique‡§ *Basinski and Basinski (1985)* [40]	The technique which avoided the stripping operation during replication procedure. Useful mainly for quantitative examination of deeper intrusions when the stripped replica can be damaged.
	Wood metal true-replica and Lacomit surface sectioning technique‡§ *Basinski and Basinski (1985)* [45]	The Wood metal preparations yield a view of replicated intrusions plus the shape of the PSM profile; the Lacomit preparations allow simultaneous examination of the specimen surface and quantitative study of the PSM profiles and initiated fatigue cracks on a cross section through it. They are applicable only for single crystals and not for polycrystals.
	Specimen surface observation by high resolution SEM-FEG (FESEM) (SEM equipped with field emission gun) *Polák and Kruml (1998)* [46]	Direct imaging of fine details of individual PSMs mainly in polycrystals.
	Sharp-corner polishing technique in combination with ECCI (electron channelling contrast imaging) *Ahmed, Wilkinson and Roberts (2001)* [47]	Simultaneous observation of surface relief profiles and associated dislocation substructures; suitable only for single crystals.
	FIB (focused ion beam) milling cross-sectioning technique† *Kraft et al. (2002)* [48], *Motoyashiki, Brückner-Foit and Sugeta (2007)* [49], *Polák et al. (2007)* [50]	Partially destructive technique for studying the profiles of extrusions and intrusions along the pre-selected cross-sections perpendicular to the individual PSMs and specimen surface and for simultaneous monitoring of cumulative PSMs evolution on two mutually perpendicular surfaces during cycling (expedient mainly for polycrystals). Periodic sectioning allows 3D analysis of surface relief or crack contour (FIB micro-tomography).
	***In-situ* specimen surface observation in environmental SEM (ESEM)** *Gall et al. (2004)* [51], *Biallas and Maier (2007)* [52]	Application of technique is similar to traditional SEM however ESEM facilitates observations in water vapour or other mildly corrosive environments (advantage for materials with high sensitivity to the environment) with the relatively low maximum gas pressure at room and elevated temperatures.
	***Post-mortem* and *in-situ* observation of specimen surface using a four-quadrant BSE (backscattered electron) -detector under special**	The technique is useful especially for visualisation of slip steps produced during half-cycle deformation after electropolishing with a minimum height of 2 nm. It yields

	imaging conditions *Weidner et al. (2006, 2008)* [53,54]	qualitative information about the nature of step (sharpness, trailing edge, rising edge, extrusion) without possibility of quantitative height measurements. This sensitive technique is suitable for pre-screening of grains for AFM; the method can be easily coupled with ECCI.
Photoelectron microscopy (PEM)	***In-situ* specimen surface observation** *Baxter (1988)* [55], *Baxter and McKinney (1988)* [56]	Examination of lateral elongation of PSMs via rupturing thin surface oxide film by the emerging extrusions without possibility of measurement their height; the method is not sensitive to intrusions. It needs thin anodic oxide film on the specimen surface.
Scanning acoustic microscopy (SAM)	**Specimen subsurface and surface observation** *Zhai, Lin and Xiao (1990)* [57], *Zhai, Martin and Briggs (1995)* [58], *Zhai, Briggs and Martin (1998)* [59]	SAM is applicable only on macro-PSMs due to lower lateral resolution (within one Rayleigh wavelength); high sensitivity for detecting fine secondary slip lines within them. TRAM is exploitable for profile measurements of macro-PSMs in single crystals and mainly for nondestructive measurements of the subsurface profile of small cracks (in anisotropic single crystals but not in large-grained polycrystals).
	TRAM (time-resolved acoustic microscopy) measurement of PSM profiles *Zhai, Martin and Briggs (1995)* [58], *Zhai, Briggs and Martin (1998)* [59]	
Scanning tunneling microscopy (STM)	**Specimen surface observation** *Venkataraman et al. (1990)* [60], *Sriram, Fine and Chung (1990)* [61], *Grosskreutz, Bowles and Wahab (1992)* [62], *Ishii et al. (1993)* [63]	3D image of surface; high resolution obtainable for measuring z-axis displacements (height of extrusions); lateral resolution is dependent on the tip geometry and specific surface relief configuration. Imaging is limited to electrical conductive materials; high sensitivity to thin oxide films on the specimen surface.
Atomic force microscopy (AFM)	**Specimen surface observation** *Harvey, March and Gerberich (1994)* [64], *Nakai, Fukuhara and Ohnishi (1997)* [65]	Quantitative 3D study of the growth of extrusions (metallic specimen) and intrusions (plastic replica) in great variability of materials (in coupling with EBSD also with respect to the crystallographic orientation of individual grains of polycrystals). The height of extrusions or the depth of intrusions is imaged truly; their real shape can be more or less laterally distorted due to specific geometry of extrusion-intrusion pairs and finite geometrical dimensions of AFM tip. Both observations (specimen + replica) are necessary to obtain true quantitative data about the simultaneous growth of extrusions and intrusions.
	Specimen surface observation in combination with EBSD (electron backscattering diffraction) *Man et al. (1999)* [66], *Sabatier, Villechaise and Girard (2000)* [67]	
	Observation via plastic replica *Nakai, Ohnishi and Kusukawa (1999)* [68]	
	Simultaneous observation specimen surface and its inverse copy obtained via plastic replica *Polák et al. (2003)* [69,70]	

‡ The technique is destructive for a fatigued specimen which does not permit the sequential observation of evolution of PSM topography during cycling.
§ Original experimental technique developed exclusively only for the purpose of quantitative study of PSM profiles and fatigue crack initiation.
† Thin foils prepared by FIB technique from surface of fatigued polycrystalline specimen have not been studied by TEM up to the present time.
3D = three-dimensional.

Table 2. Comparison of models of surface relief evolution leading to transcrystalline fatigue crack initiation in f.c.c. single- and polycrystals.

Model	Applicability‡	Origin of cracks	Criterion of fatigue crack initiation
Brown and co-workers (1976 and later)	individual PSBs in S and P, macro-PSBs in S	surface decohesions opened due to logarithmic infinities in stress developed at sites where PSB-matrix interface meets external surface	not specified
EGM+DEM (1981+1986)	individual PSBs in S and P	surface shear decohesions due to stress raisers type I (steep flanks of extrusion; i.e. crack initiation along PSB-matrix interface) or II (notch-like valleys within the profile of PSM)	not specified
Polák (1985, 1987 and later)	individual PSBs in S and P, macro-PSBs in S	intrusions accompanying extrusion and/or protrusion in a characteristic way (for PSM geometry see figure 2)	the rate of new surface (crack) formation due to stress concentration and/or slipping-unslipping is higher than intrusion growth rate given by the local strain amplitude and the resulting vacancy generation and migration rates
Lin and his associates (1969 and later)	thin individual PSBs in S and P	individual intrusion	not specified
Mura and co-workers (1981 and later)	very thin individual PSBs in P	individual intrusion or subsurface initiation at grain boundary at the site of contact point with PSB connected with extrusion on the specimen surface	energetic – critical value of the stored strain energy of accumulated dislocations
Rosenbloom and Laird (1993)	macro-PSBs in S	valley in macro-PSM profile	geometrical – the presence of a 4 μm peak or valley in macro-PSM profile
Repetto and Ortiz (1997)	individual PSBs in S and P	intrusions accompanying extrusion along PSB/matrix interface	geometrical – sharpening of intrusions (grooves) into the form of a mathematically sharp cracks defined by zero angle between the sides of groove at its apex
Déprés et al. (2004 and later)	individual PSBs in S and P	intrusions accompanying extrusions (along PSB-matrix interface or within PSMs)	energetic – critical value of local dislocation distortion energy within the channels of PSB due to stress tri-axiality

‡ S = single crystal, P = polycrystal; for typical individual PSB and macro-PSB see figure 2.

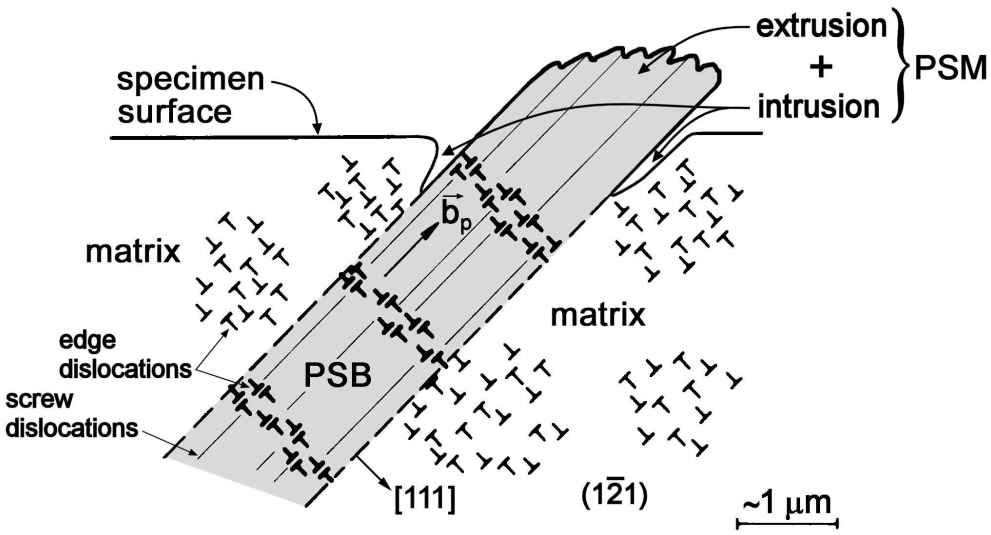

Figure 1. Section through the grain showing surface profile of mature PSM formed at the side where PSB intersects free surface. The dislocation distributions in PSB with so-called ladder structure embedded in the matrix with vein structure are indicated schematically according to Essmann et al. [18]. Dipolar nature of the walls in PSB is highlighted in agreement with Antonopoulos et al. [19].
86x47mm (600 x 600 DPI)

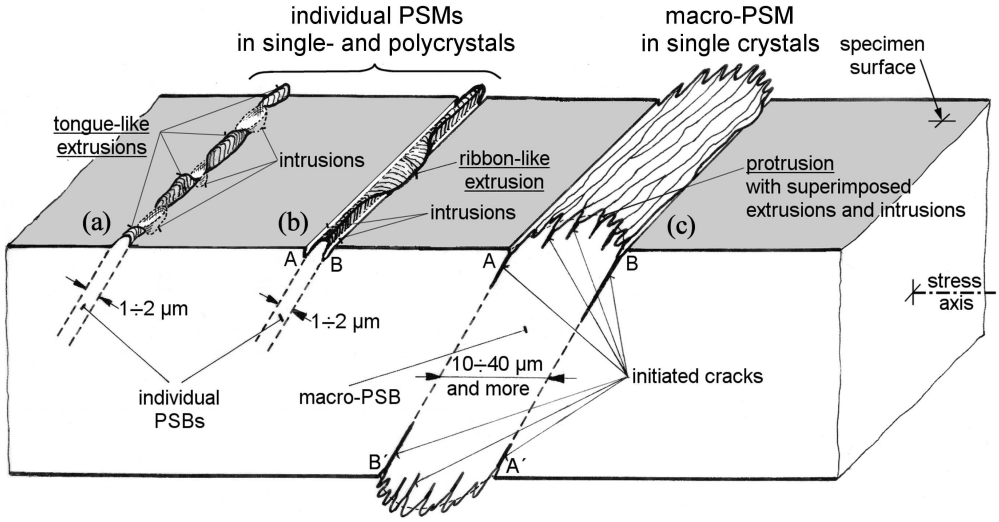

139x73mm (500 x 500 DPI)

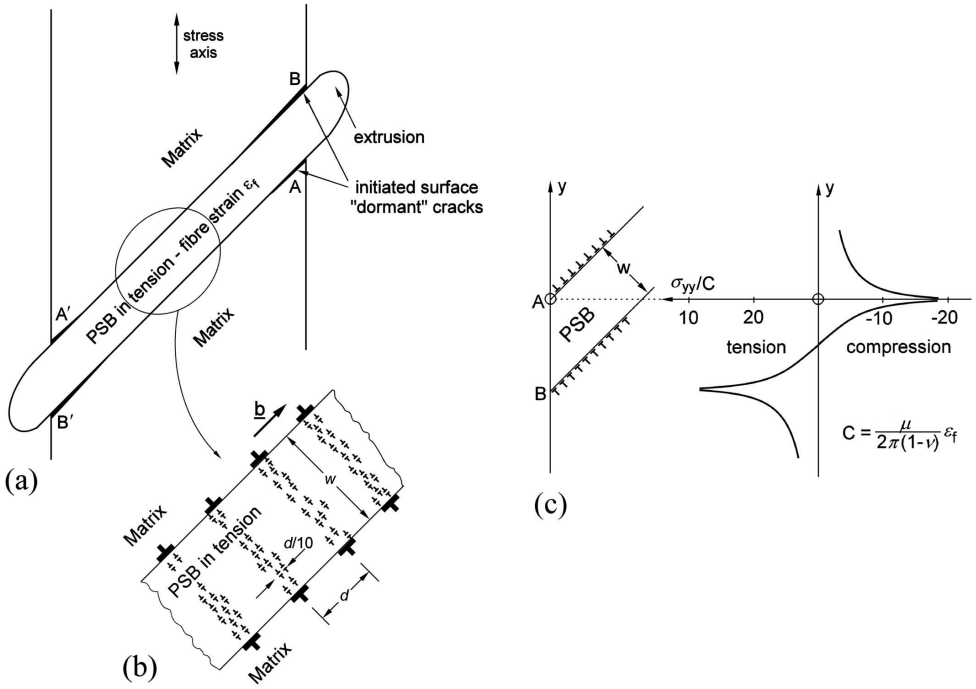

92x64mm (600 x 600 DPI)

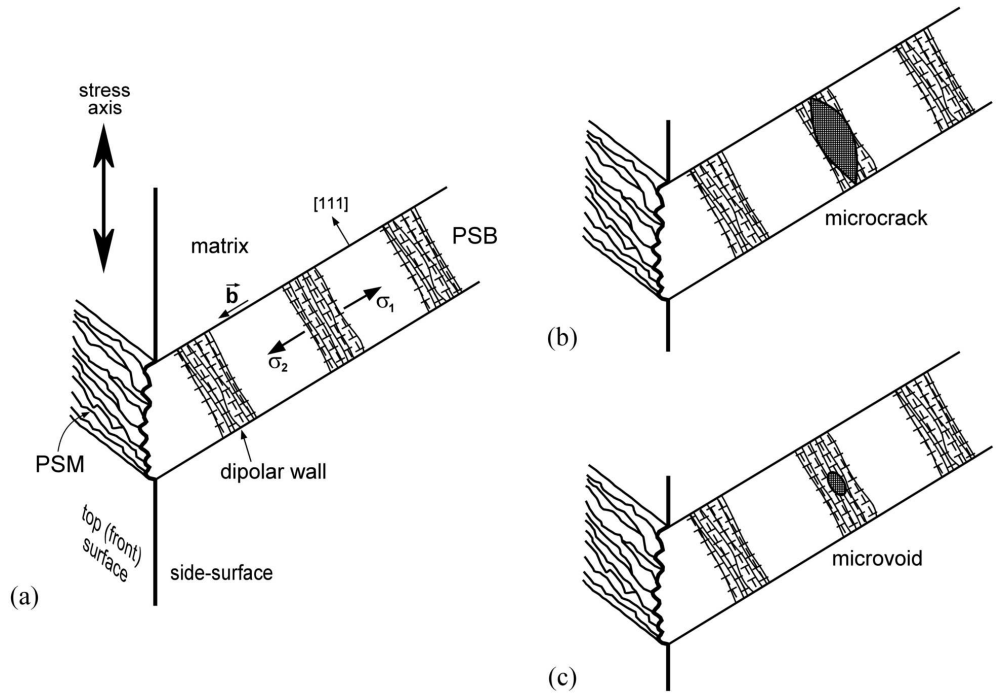

Figure 4. Model of microcrack initiation in a PSB on the side surface containing Burgers vector by Zhai et al. (schematically). (a) A dipolar dislocation wall in the PSB is under a resulting internal tensile stress mainly caused by massive irreversible slip carried by screw dislocations in the surface region. (b) A microcrack initiation from the dislocation wall in the PSB due to the collapse of the wall under the joint action of the internal tensile stress $\sigma_1+\sigma_2$ and the applied stress. (c) Possible formation of a microvoid due to only a partial collapse of the wall provided the internal tensile stress $\sigma_1+\sigma_2$ is not uniform along the wall. After [57,58]. *(Reprinted with permission from Elsevier)*
83x58mm (600 x 600 DPI)

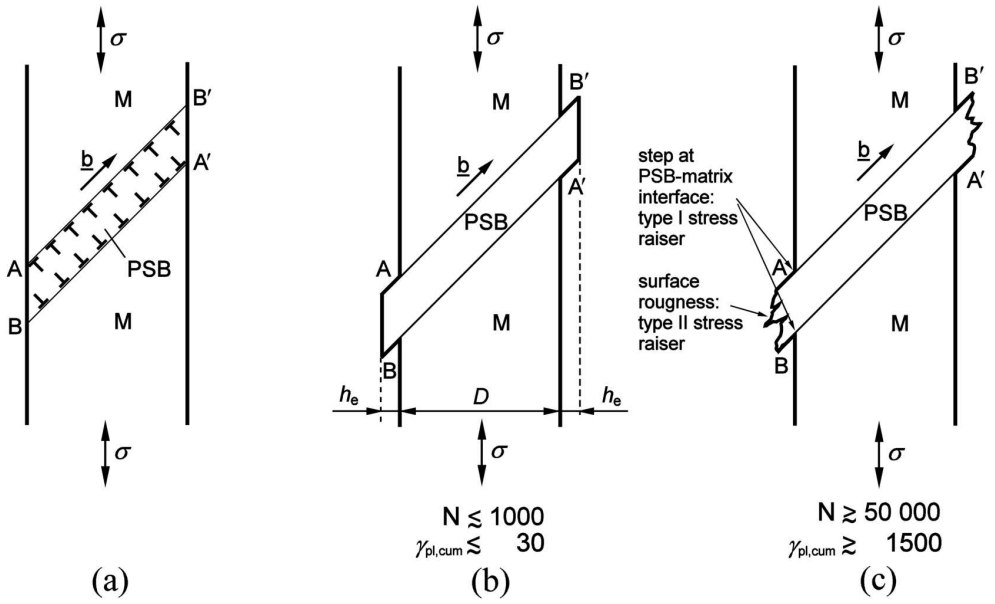

Figure 5. Model by Essmann, Gösele and Mughrabi (EGM-model) of PSB surface profile formation (schematically). (a) Accumulation of PSB-matrix interface dislocations. (b) Rapid formation of static extrusion after emergence of interface dislocations. (c) Slow roughening of the profile of the static extrusion by random slip with indicated two types of the stress raisers considered by EGM for fatigue crack nucleation. **b** – Burgers vector, M – matrix, PSB – persistent slip band, N – number of cycles, $\gamma_{pl,cum}$ – cumulative plastic shear strain. After [18,81]. *(Adapted from [81]. Copyright © 1985 by The Institute of Metals, London. Reprinted by permission from The Institute of Materials, Minerals and Mining)*
71x43mm (600 x 600 DPI)

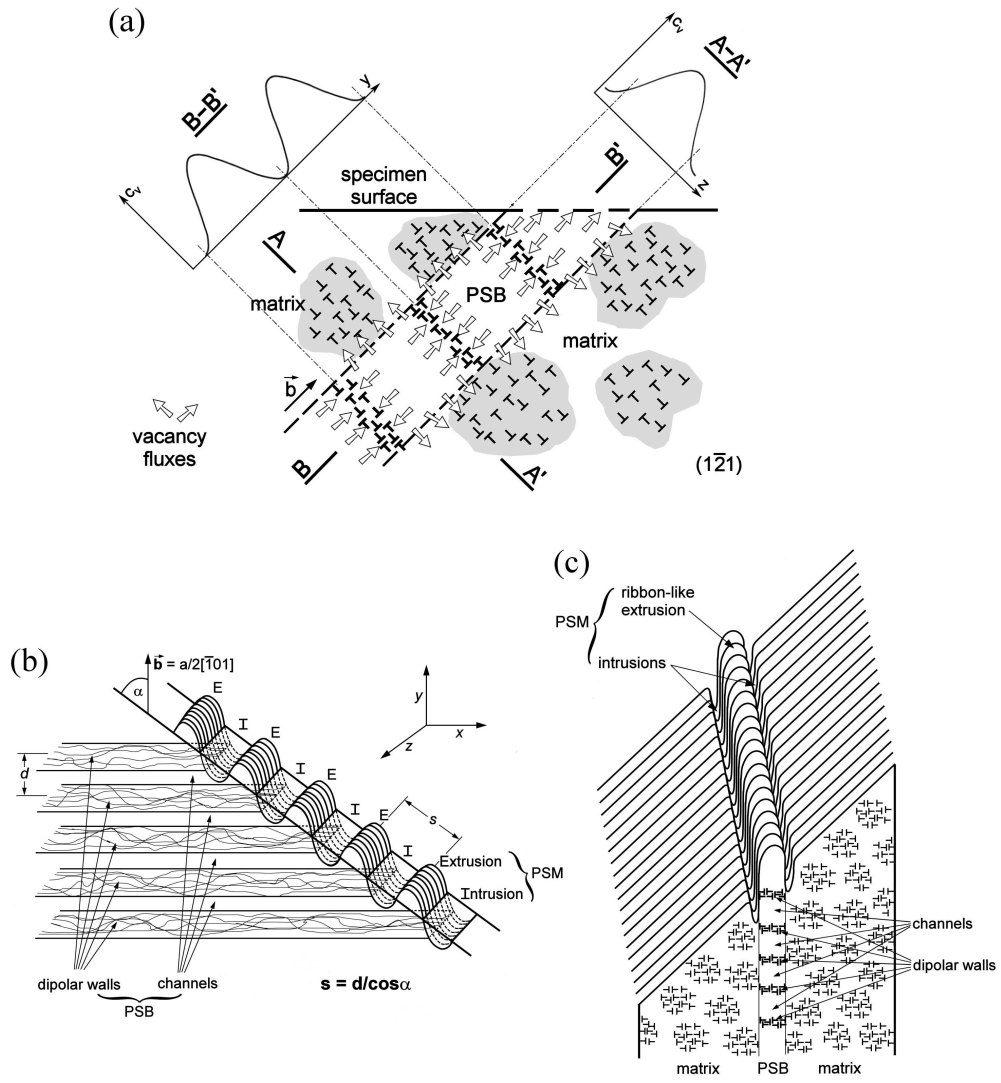

Figure 6. Polák's model of surface relief formation for an individual PSB. (a) Schematic section through a crystal containing PSB and matrix in a plane and quasi-stable vacancy concentration profiles within PSB (section) and in a plane perpendicular to PSB (section) in constant frequency cycling. Vacancy fluxes within the PSB and out of the PSB are indicated by arrows. (b) Relation (schematic) between the dislocation structure of a PSB and adjacent PSM when the point defects migrate within the band. (c) Surface profile (schematic) of a PSM when point defects migrate from the band to the matrix. *(Reprinted from [109] with permission from Elsevier)*
124x135mm (600 x 600 DPI)

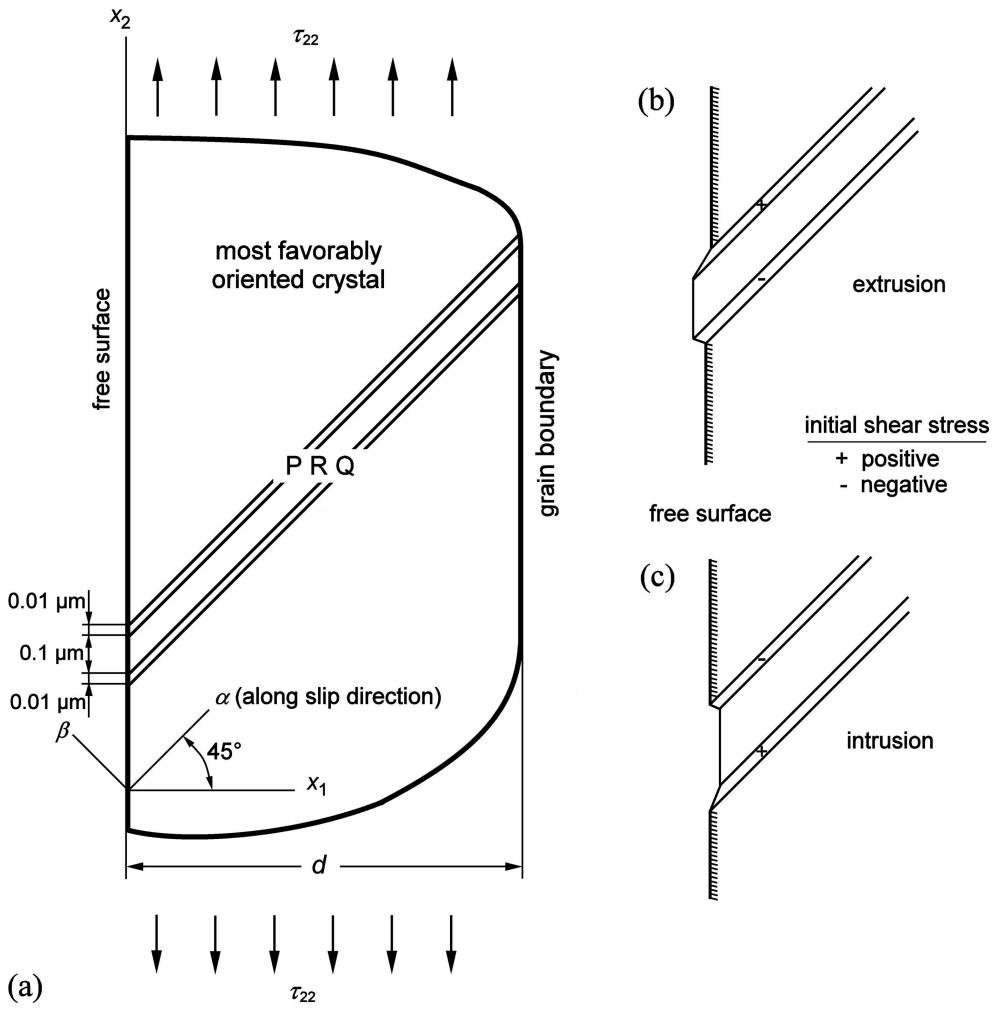

Figure 7. The micromechanical model of extrusion and intrusion formation suggested by Lin and his associates. (a) PSB in most favourably oriented grain at the free surface of a polycrystal. The slip plane and the slip direction of the most favourable slip system form an angle of 45° with the specimen axis. (b) Extrusion or (c) intrusion formed at a free surface with the indicated signs in the initial stress field in slices P and Q. After [99,118]. *(Figure 6(b) and 6(c) reprinted from [99] with permission from ASTM International)*
120x122mm (600 x 600 DPI)

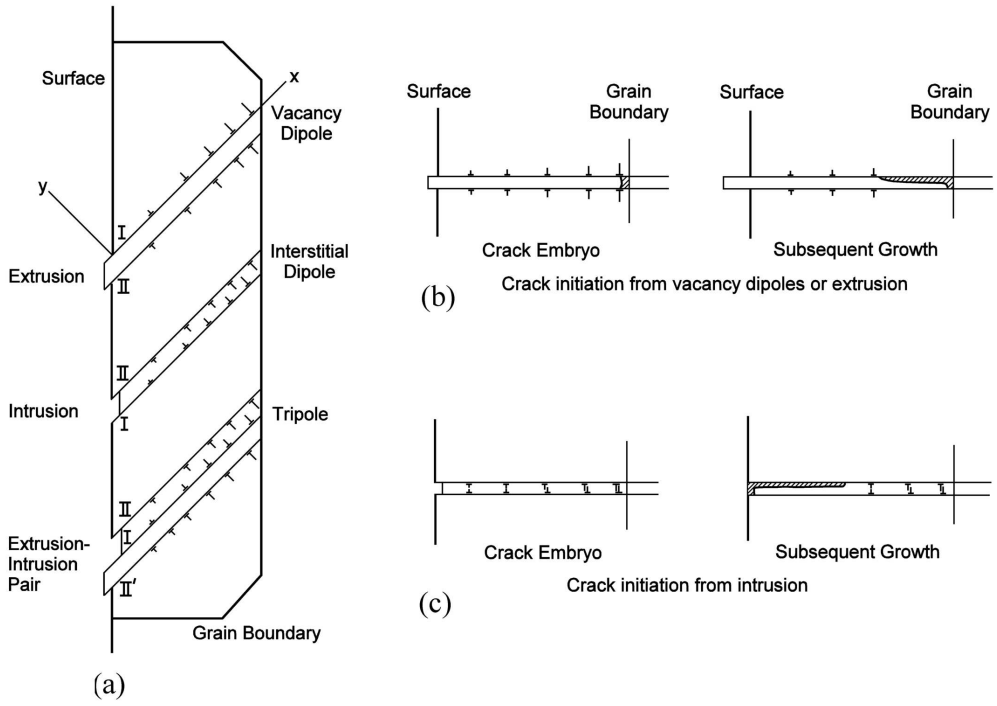

Figure 8. Model by Tanaka and Mura of surface relief formation and fatigue crack initiation in a PSB. (a) Schema of plate-like layers (PSBs) with accumulated dislocation pileups at the grain boundary in most favourably oriented grain and the formation of extrusion, intrusion or extrusion-intrusion pair shown in the section perpendicular to the specimen surface. The dislocation pileups on layers I and II are under tension and compression respectively. (b) Crack initiation from vacancy dipoles or extrusion. (c) Crack initiation from intrusion. *(Taken from [125]. Reprinted by permission of ASME)*
90x64mm (600 x 600 DPI)

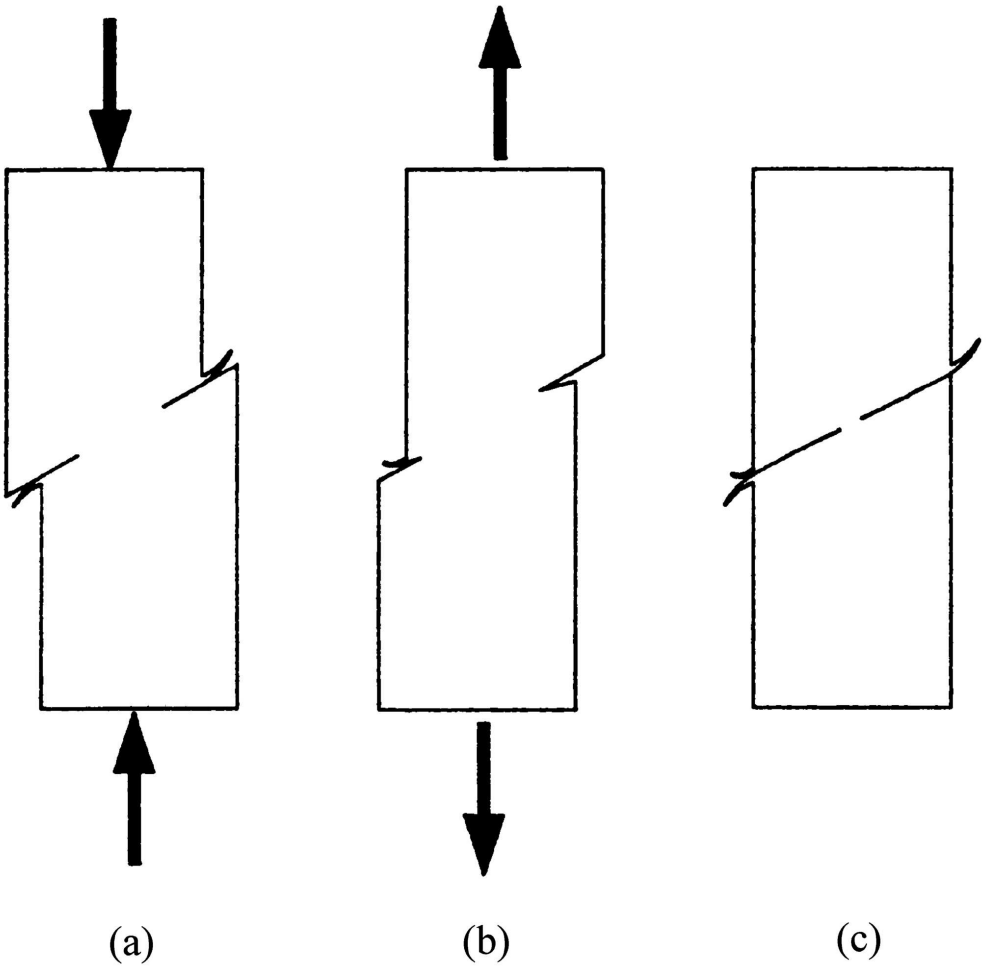

Figure 9. The crack closure-fracture surface rubbing (CCFSR) mechanism for formation of thin extrusions in the presence of a pre-existing small crack in a single crystal suggested by Dickson et al. [131] (schematically). (a) During the compression portion of the load-decreasing half cycle, the extrusion is produced by a rubbing/burring process on the crack face which subtends an obtuse angle with the specimen surface. The fracture surface rubbing also tends to push the extrusions away from the crack. (b) During the load-increasing portion of the stress cycle, an extrusion can form on the other face, if there is sufficient local crack closure to produce the required fracture surface rubbing. (c) The net effect is that more numerous and larger extrusions are formed on the crack faces subtending an obtuse angle with the specimen surface. *(This figure originally appeared in [131], published by EMAS Publishing in 1993, ISBN: 0–947817–60–3 and is reproduced with their permission – www.emas.co.uk)*
86x84mm (600 x 600 DPI)

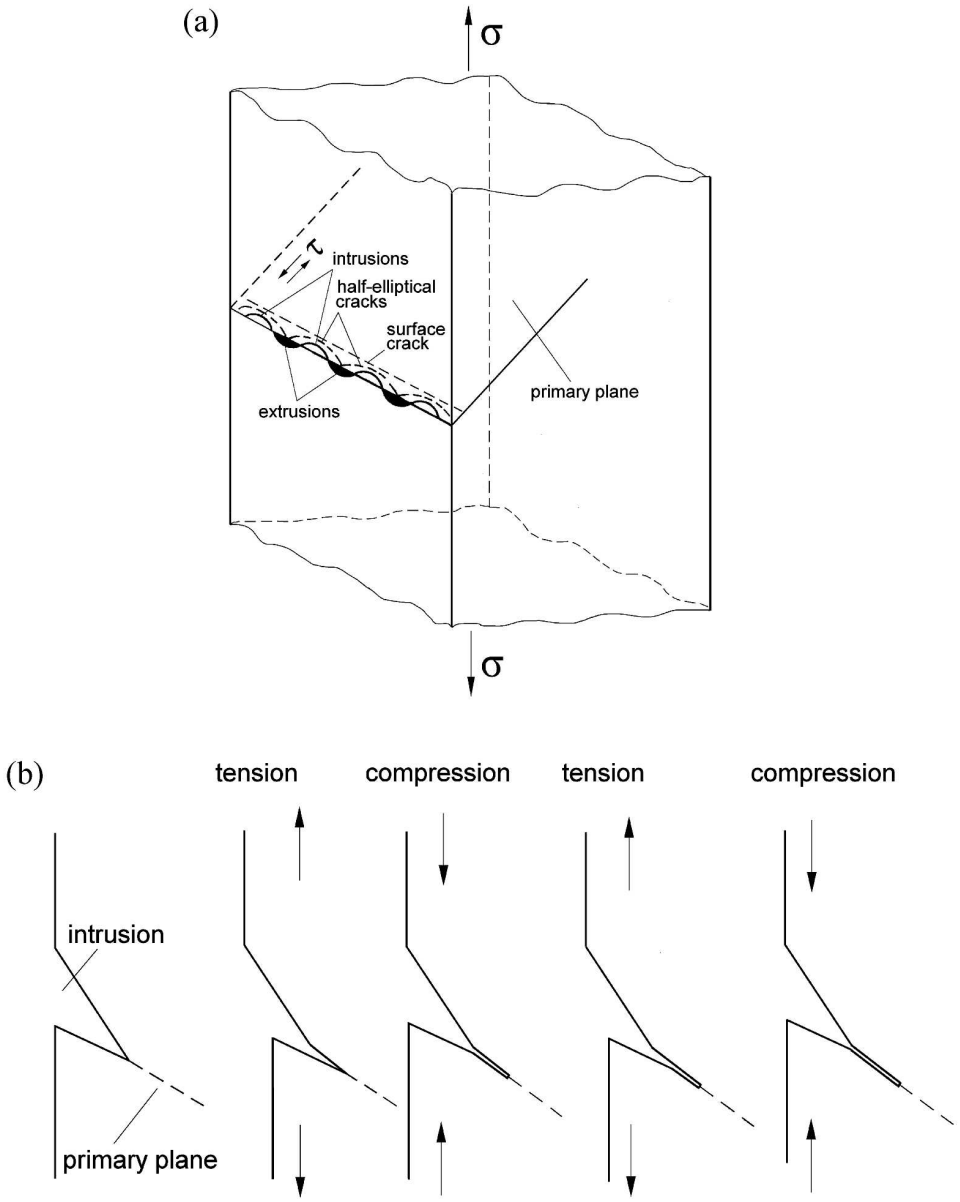

Figure 10. (a) Mechanism of crack nucleation from a row of intrusions quasi-periodically alternating with tongue-like extrusions. (b) Environmentally assisted slip-unslip mechanism leading to crack growth from an intrusion parallel to ribbon-like extrusion (not shown in figure) along the PSB-matrix interface. *(After figure 10 in [84]. Reprinted by permission of Blackwell Publishing)*
132x166mm (600 x 600 DPI)